Dr. Thorsten Bartels-Rausch
Co-Editor of Atmospheric Chemistry and Physics

Dear Dr. Bartels-Rausch,

Given below are our responses to the comments provided by the reviewers of our manuscript. For clarity, the referee comments or questions are in black text, and are preceded by bracketed, italicized numbers (e.g. *[1]*). Our (authors') responses are in in blue text below each comment or question with matching italicized numbers (e.g. *[A1]*). The revised text according to each referees' comment or question is in green text below each authors' response, with corresponding page and line numbers in the original manuscript (e.g. *[R1, page 1 lines 1-2]*). We thank the reviews for their time and care reading our manuscript and for their helpful comments and questions.

Sincerely,

Allan Bertram
Professor of Chemistry
University of British Columbia

Anonymous Referee #1

Summary:
The authors present measured diffusivities of tracers in three proxies for secondary organic aerosols. They have compared their observations with predictions based on the Stokes-Einstein relation. From their measurement data, they have presented parameters for a fractional Stokes-Einstein relation. They have also compared their observations with observations in literature and predictions from Stokes-Einstein relation and their model for a fractional Stokes-Einstein relation. The experiments seem properly done and are simply and clearly explained. Their data are also simply and clearly presented. There are however a few questions I would like answered:

Major comments:
[1] There is a comparison between their developed fractional Stokes-Einstein relation and the Stokes-Einstein relation. Price et al. (2016) already presented a fractional S-E relation. A comparison of their outcome with this model was not made. Do we really need a new fractional S-E relation when that from Price et al. already exists? How does Price et al.'s compare to your model and your observations? What does C in the fractional relation represent?
[A1] Regarding the first part of this comment, the fractional Stokes-Einstein relation from Price et al. 2016 was derived using only diffusion data of sucrose in sucrose-water matrices. The new fractional Stokes-Einstein relation was derived using diffusion data of several large organic molecules in several types of organic water-matrices. To address the referee's comments, in the revised manuscript we will add a direct comparison between the new fractional Stokes-Einstein relation, and the fractional Stokes-Einstein relation derived by Price et al. (2016).

Regarding the second part of this comment, the C in the fractional Stokes-Einstein relation is related to ξ and the crossover viscosity (η_c), specifically, $C=\eta_c^{\xi}/\eta_c$. The crossover viscosity is the viscosity at which the Stokes-Einstein relation and the fractional Stokes-Einstein relation predict the same diffusion coefficient. Based on the data in Fig. 3 we have chosen $\eta_c = 10^{-3}$ Pa s.

For clarity we have decided to re-write the fractional Stokes-Einstein relation to eliminate the variable *C*. An alternative way to write the fractional Stokes-Einstein relation is:

$$D = D_c \left(\frac{\eta_c}{\eta}\right)^{\xi}$$

where ξ is the same empirical parameter as in the previous version of the fractional relation, η_c is the crossover viscosity, and D_c is the crossover diffusion coefficient. The crossover viscosity corresponds to the viscosity at which the system changes from one that follows the Stokes-Einstein relation to one that follows the fractional Stokes-Einstein relation. The crossover diffusion coefficient corresponds to the diffusion coefficient at η_c (which can be calculated with the Stokes-Einstein relation). The following changes were made to the text and all references to the variable *C* have been removed.

[R1, page 9 line 3] This is in close agreement with the findings of Price et al. (2016) who showed that the diffusion of sucrose in a sucrose-water matrix could be modelled using a fractional Stokes-Einstein relation with ξ = 0.90 over a large range in viscosity. The new fractional Stokes-Einstein relation, which builds on the work of Price et al. (2016), was derived using diffusion data of several large organic molecules in several types of organic water-matrices, and thus demonstrates a broader utility of the fractional Stokes-Einstein relation.

[R1, page 8 line 23] Building on that work, the data in Fig. 3a were fit to the following fractional Stokes-Einstein relation:

~~$D = C\frac{kT}{6\pi\eta^{t}R_H}$~~ $D = \left(\frac{\eta_c}{\eta}\right)^{\xi}$

where ~~*t* and *C* are~~ ξ is an empirical fit parameter~~,~~. ~~s.~~ η_c is the crossover viscosity, and D_c is the crossover diffusion coefficient. The crossover viscosity is the viscosity at which the Stokes-Einstein relation and the fractional Stokes-Einstein relation predict the same diffusion coefficient. Based on the data in Fig. 3 we have chosen $\eta_c = 10^{-3}$ Pa s. The crossover diffusion coefficient corresponds to the diffusion coefficient at η_c (which can be calculated with the Stokes-Einstein relation). The value of ξ is determined as the slope of the dashed line in Fig. 3a. ~~When fitting Eq. 3 to the data, we used the additional constraint that log (D) – log (kT/6πRH) equals 3 when the viscosity is 10-3 Pa s, which is equivalent to assuming the Stokes-Einstein relation is valid at a viscosity of 10-3 Pa s (roughly the viscosity of water).~~ The best fit to the data (represented by the dashed line in Fig. 3a) resulted in a ~~*t*~~ξ value of 0.93~~ and a *C* value of 1.66~~.

[2] What saturated salts were used in setting the relative humidity and what is the water activity over those salts used? This can be presented as part of the SI.
[A2] A new table has been added to the SI (Table S1) which lists the salts used and the relative humidity of the air space measured above each salt.

[3] Crystallization in the droplets: was there a control sample without the tracers? How does the occurrence of crystallization at the low water activity in droplets without tracers compare to droplets with the tracers? A statement of how the tracers impact the behaviour of the test solution should be made.
[A3] We did not condition a control sample without fluorescent organic molecules to experimental a_w in order to determine the effect of the tracer on the crystallization of the droplets. However, pure solutions (of the organic matrix molecules and water studied here) can exist as supersaturated droplets at the same water activities as studied here without crystallizing. We know this because droplets in the metastable supersaturated (non-crystalline) phase are required to generate the viscosity data given by the literature viscosity sources. Furthermore, since the concentrations of the tracers in the droplets were so low, the

tracers are not expected to change the driving force for crystallization in the droplets. The following has been added to the text.

[R3, page 5 line 6] We did not condition droplets without fluorescent organic molecules to determine the effect of the tracer molecules on crystallization. However, previous studies have shown that droplets with the compositions and range of a_w values studied here can exist in the metastable liquid state if heterogeneous nucleation by surfaces is reduced. Furthermore, since the concentration of the tracers in the droplets were so low, the tracers are not expected to change the driving force for crystallization in the droplets.

Minor comments:

[4] Please include a "," after following on line 8, page 3

[R4, page 3 line 8] In the following, we expand on the previous studies with sucrose matrices…

[5] Please include a "," before "we account..." on line 12, page 7

[R5, page 7 line 12] By plotting log (D) – log ($kT/6\pi R_H$), we account for differences in hydrodynamic radii…

[6] Please include a "," after "In Fig 3a on line 30, page 7

[R6, page 7 line 30] In Fig. 3a, we have combined the results from the current study…

[7] Please change "t" as the symbol for the fractional parameter in the fractional S-E relation; "t" has been used elsewhere in the paper to represent time.

[A7] We have replaced the variable "*t*" with the symbol "*ξ*" for the exponent in the fractional Stokes-Einstein relation.

Anonymous Referee #2

Summary:

In this work the authors present measurements of the diffusion coefficients of a fluorescent organic tracer in secondary organic aerosol proxy compounds (citric acid, sorbitol, and a sucrose-citric acid mixture). They compare their measured diffusion coefficients with the predicted diffusion coefficients by the Stokes-Einstein relation. From this comparison they propose a parameterization of a fractional Stokes Einstein relation. The suggested fractional Stokes-Einstein relation seems to be a better model for predicting diffusion coefficients in SOA proxies, for the range of viscosities studied. The comparison is made as well for earlier work. The writing is clear and the data is presented in a comprehensive and clear way. This work is of a great interest for the atmospheric science community and it is definitely suitable for publication in ACP. I would raise only few minor comments.

Comments:

[8] How dependent of the nature of the diffusing molecule are the parameters t and C? In the experiments the diffusing molecule was rhodamine 6D, which is quite a large molecule. How would the parameters change for smaller molecules?

[A8] A strong relationship between the size of the diffusing molecule and the parameter *t* (now *ξ* in this work) is suggested by Price et al. (2016), who report values of *t* for both sucrose and water molecules diffusing in a sucrose-water matrix. Here we focus on providing a fractional Stokes-Einstein relation that is applicable to cases where the size of the diffusing molecule is equal to or larger than the organic molecule in the matrix. For this case, a strong relationship between the size of the diffusing molecule or the nature of the diffusing molecule was not observed. Ongoing work in our laboratory is exploring the

relationship between *t* and the size of the diffusing molecule when the size of the diffusing molecule is smaller than the organic molecule in the matrix. We have changed "organic molecules" to "large organic molecules" in the title, and added the following text to the manuscript.

[R8, page 9 line 3] For the case of large diffusing molecules such as those included in this work (i.e. the radius of the diffusing molecule is equal to or larger than the radius of the organic molecules in the matrix), we do not observe a strong dependence of ξ on the size or nature of the diffusing molecule. For smaller molecules, ξ is expected to change significantly. For example, Price et al. (2016) showed that ξ = 0.57 for the diffusion of water in a sucrose-water matrix, and Pollack (1981) showed that ξ = 0.63 for diffusion of xenon in a sucrose-water matrix. The development of a relationship between ξ and the size of small diffusing molecules is beyond the scope of this work.

[9] Line 21, page 1."...measured diffusion coefficients over eight orders in magnitude...". Diffusion coefficients of what? I would write "diffusion of coefficient of organic compounds" or something similar.
[A9] The text has been modified as follows.
[R9, page 1 line 21] We measured diffusion coefficients of large organic molecules over eight orders in magnitude in proxies of SOA.

[10] I would include in the abstract how the diffusion coefficients were measured (fluorescence, rhodamine 6G...).
[A10] The description of the measurement technique has been added to the abstract.
[R10, page 1 line 22]). However, the accuracy of this relation for predicting diffusion in SOA remains uncertain. We measured diffusion coefficients over eight orders in magnitude in proxies of SOA including citric acid, sorbitol, and a sucrose-citric acid mixture. Diffusion coefficients of two fluorescent organic molecules, rhodamine 6G and cresyl violet, were measured using rectangular fluorescence recovery after photobleaching (rFRAP).

[11] Is the photobleaching affecting the temperature of the films?
[A11] The photobleaching is not expected to affect the temperature of the thin films in such a way that measured diffusion coefficients would be affected. The following text has been added to the manuscript.

[R11, page 5 line 21] The energy absorbed by the thin film during photobleaching is not expected to affect measured diffusion coefficients. Although local heating may occur during photobleaching, the thermal diffusivity in the samples is orders of magnitude greater than the molecular diffusivity, and the heat resulting from photobleaching will dissipate to the surroundings on a timescale much faster than the diffusion of molecules will occur (Chenyakin et al., 2017). Measurements as a function of photobleaching size and power are consistent with this expectation (Chenyakin et al., 2017; Ullman et al., 2019).

Anonymous Referee #3

Summary:
The manuscript submitted to Atmospheric Chemistry and Physics titled "Predictions of diffusion rates of organic molecules in secondary organic aerosols using the Stokes-Einstein and fractional Stokes-Einstein relations" by Evoy et al. presents diffusion coefficients, D, and viscosity, η, of fluorescent dyes in organic compounds, which are proxies of secondary organic aerosol (SOA) material. Using their data and data from previous studies, they test the applicability of the Stokes-Einstein (SE) relation. The authors find that although the SE relation is fairly accurate within their experimental uncertainty, a better fit could be made

using a fractional Stokes-Einstein (FSE) relationship, with 2 fit parameters to adjust the linear relationship between ln D versus ln η. The authors compare the SE and FSE relation in terms of mixing times, τ, calculated for particles 200 nm in diameter as a function of latitude and pressure levels in the atmosphere. The authors conclude that when η is high, τ and D calculated using the FSE are up to 10 times shorter. Overall, this manuscript adds to the growing database of D and η for many atmospherically relevant compounds and proxies. The methods are accurate and the error analysis is justified. Finally, the results and implications are presented clearly. I will add that this manuscript was a pleasure to read and review. There is one major comment about how previous literature is described by the authors. A few minor comments must also be addressed before I can recommend publication. Page and line numbers are indicated below, and all references are taken from the manuscript.

Major Comments:

[12] p. 2, l. 13-17: The authors use these sentences to claim importance of SOA growth, mass, chemical reactivity and photochemical reactivity. These statements are valid but for a limited range of conditions. The authors should state what range of D or η these are actually valid, or readers not in the field may be misled. Specific examples should be given here to reveal to the reader when diffusion limitations significantly affect atmospheric processes such as SOA growth or photochemical reactions and when they do not. This paragraph can be extended to discuss these details. I will only discuss a few references below, and implore the authors to recheck all cited previous publications here for the conditions of D and equilibrium timescales, τ, that are important for SOA formation and (photo)chemical reaction.

- Shiraiwa and Seinfeld (2012): Measurements in this manuscript are for10−15−10−6cm2s−1. However, Shiraiwa and Seinfeld (2012) show that values of τ are unchanging when D is varied between about10−15−10−5cm2s−1. This says to me that changes in D are not important at all to τ for their observations, and thus not important to SOA growth. It can be important for a lower range of D and a specific particle size, however these details are not included in the manuscript. This should change in the introduction.
- Zaveri et al. (2018): In Figs. 4 and 5 of Zaveri et al. (2018), size changes for SOAparticles ≥ 200nm in diameter could be successfully modeled using both liquid-like and semi-solid scenarios. This would lead to the conclusion that, changing D and τ for 200 nm particles shown in Fig. 5 of this submitted manuscript would not make any difference to SOA size or mass. This is contrary to what they write.
- Hinks et al. (2016): How does viscosity change light absorption and quantum yield of a photochemical reaction rate? Excitation reaction R1 in Hinks et al. (2016) is not altered by changing D. Therefore, the statement that “photochemistry” depends on D is incorrect. However, chemical reactions R2-R4 could be diffusion limited. These details should be stated, otherwise this statement can mislead readers.

[A12] To address the referee’s comments, we have qualified many statements in the text relating to the importance of diffusion for predicting SOA growth, reactivity, and the long-range transport of pollutants. References relating to photochemistry have been removed. The reference relating to predictions of SOA mass has also been removed. The following illustrates the modifications made to the text.

[R12, page 2 line 13] ~~For example, predictions of SOA mass, which has major implications for climate and air quality, can vary by an order of magnitude when the molecular diffusion rate of organic molecules in SOA is varied in models (Shiraiwa and Seinfeld, 2012).~~

[R12, page 2 line 15] For example, predictions of SOA particle size, which has implications for climate and visibility, ~~also~~ varies significantly in simulations as the diffusion rate of organic molecules is varied from 10^{-17} to 10^{-19} m^2 s^{-1} (Zaveri et al., 2014~~, 2018~~)

[R12, page 2 line 17] Lifetimes of polyaromatic hydrocarbons (PAHs) in an SOA particle increase as the bulk diffusion coefficient of PAHs decreases from 10^{-16} m^2 s^{-1} at a relative humidity of 50% to 10^{-18} m^2 s^{-1} under dry conditions (Zhou et al., 2019). Shrivastava et al. (2017) have shown that including shielding by a viscous organic aerosol coating (equivalent to a bulk diffusion limitation) results in better model predictions of observed concentrations of PAHs.

[R12, page 2 line 17] Reactivity ~~and photochemistry~~ in SOA can also depend on diffusion rates of organic molecules (Davies and Wilson, 2015; ~~Hinks et al., 2016;~~ Lakey et al., 2016; Li et al., 2015; ~~Lignell et al., 2014;~~ Liu et al., 2018; Shiraiwa et al., 2011; Zhang et al., 2018; Zhou et al., 2013). For the cases discussed above, diffusion of organic molecules within SOA becomes a rate-limiting step only when diffusion rates are small.

Minor Comments

[13] p. 1, l. 20-21: The authors did not measure D. They measured the change inflorescence intensity over time. D was derived from fitting their florescence intensity measurements, and then fitting again their fitted parameter (r2+4Dt) over time (p. 6, l. 9 and 15). Please search for all instances of the phrase "measured diffusion coefficients" or similar and rephrase.

[A13] We have either replaced the phrase "measured diffusion coefficients" with "determined diffusion coefficients," "experimental diffusion coefficients," or else have deleted the word "measured" throughout the manuscript.

[14] p. 1, l. 27-28: The authors make the claim that differences in D between the SE and FSE relation can be important for predicting SOA particle size and chemical reaction rates. SOA size or reaction rates were not measured or modeled in this manuscript and so this sentence misleads readers. This is more of an introductory sentence than a consequence determined by their results. This sentence should be included in the beginning of the abstract and reworded for clarity.

[A14] This sentence has been moved to the beginning of the abstract and reworded.

[R14, page 1 line 18] ~~These differences~~Diffusion can be important for predicting growth, evaporation, and reaction rates of SOA under certain atmospheric conditions.~~in the middle and upper part of the troposphere.~~

[15] p. 1, l. 28-29: This sentence is a very unusual way to end an abstract. What I read here is that the diffusion results are important when diffusion is important. This is a very weak sentence and suffers circular reasoning. Please rephrase.

[A15] The final sentence of the abstract has been modified as follows.

[R15, page 1 line 28] These results also have implications for other areas where organic water-matrices are important, such as in food sciences and the preservation of biomolecules.~~diffusion of organic molecules within organic-water matrices is important.~~

[16] p. 6. l. 8 and Equation 2: I am confused about how the fitting was done, likely because of Fig. S6. Was a time evolving surface fit (2-D) performed? Was the data first averaged as in Fig. S6, and then fit in 1-D? Please briefly clarify what was actually fit in the text.

[A16] Equation 2 was fit to the full images (128x128 pixels following downsizing) to determine the diffusion coefficients. Figure S6 is included only to allow the reader to visualize the fit of the equation to the data. The text has been modified in two places to clarify.

[R16, page 6 line 8] The entire images (128x128 pixels following downsizing) collected during a rFRAP experiment were fit to Eq. (2) using a Matlab script...

[R16, page 6 line 20] Figure S6 is given only to visualize the fit of the equation to the data, and the cross-sectional fit was not used to determine diffusion coefficients. As mentioned above, the entire images (128x128 pixels following downsizing) were used to determine diffusion coefficients.

[17] Figure S6: I question why averaging over the y-direction was used here. The corners of the bleached rectangle should "round" as time progresses (Fig. S4e), and the spot then appears more like a circle. Therefore, can averaging over the y-direction really be called a cross-section? Would the authors agree that showing a measured 2-D surface intensity plot and modeled lines of constant intensity would be more beneficial to understand the measurements and fit?
[A17] Averaging over the width of the bleach in the y direction was done to demonstrate to the reader, using Fig. S6, that the bleach depth is initially roughly 30% and decreased over time as diffusion of fluorescent molecules occurred. We believe this is easier to visualize using an intensity profile rather than a surface intensity plot.

[18] p. 8, l. 17-18: I am pleased that the authors have not oversold themselves here and used words like "suggest" and "may". Throughout their manuscript, their data and analysis has been worded very well.
[A18] No changes have been made in terms of the wording of the data and analysis. Qualifying words such as "suggest" and "may" have been maintained.

[19] p. 9, l. 1-3: Is this too obvious? More fitting parameters will always give a better fit. Is a quantitative metric to evaluate whether or not the data are consistent with a certain model? As it is written, the authors want the reader to look at the residuals in Fig. 3b) and c) and come to the same qualitative reasoning. I would recommend a simple chi-squared test to give quantitative evidence and strengthen their claim.
[A19] A reduced chi-squared test has been used to strengthen the claim that the data are more consistent with the fractional Stokes-Einstein relation compared to the Stokes-Einstein relation. The following has been added to the text.
[R19, page 9 line 1] Beyond the sum-of-squared residuals test we have performed a reduced chi-squared (χ^2) test which takes into account the extra fitting variable present in the fractional Stokes-Einstein relation. Assuming a variance of 0.25, the reduced χ^2 value is 1.24 for the Stokes-Einstein relation and is 0.67 for the fractional Stokes-Einstein relation.

[20] Figure 3a and Eqn 3: When the authors fit to the FSE relation, did they consider a weighted fit to the uncertainties? I could imagine some data points by different authors are more certain than others. Please state in the manuscript if the fit was weighted with any uncertainties.
[A20] The fit to the data in Figure 3a given in Equation 3 was not weighted with any uncertainties. This is in part because precise uncertainties were not given in all literature sources. The text has been updated to reflect that the data were not weighted using uncertainties.
[R20, page 8 line 29] Each data point was weighted equally when performing the fitting.

[21] From the journal website, "Authors are required to provide a statement on how their underlying research data can be accessed. This must be placed as the section "Data availability" at the end of the manuscript before the acknowledgements." Please fulfill this data policy requirement.
[A20] The following statement has been added to the manuscript.
[R20, page 11 line 3] Underlying data and related material for this paper are located in the Supplement.

Predictions of diffusion rates of large organic molecules in secondary organic aerosols using the Stokes-Einstein and fractional Stokes-Einstein relations

Erin Evoy[1], Adrian M. Maclean[1], Grazia Rovelli[2,a], Ying Li[3], Alexandra P. Tsimpidi[4,5], Vlassis A. Karydis[4,6], Saeid Kamal[1], Jos Lelieveld[4,7], Manabu Shiraiwa[3], Jonathan P. Reid[2], and Allan K. Bertram[1]

[1] Department of Chemistry, University of British Columbia, 2036 Main Mall, Vancouver, BC, V6T 1Z1, Canada
[2] School of Chemistry, University of Bristol, Bristol, BS8 1TS, UK
[3] Department of Chemistry, University of California, Irvine, California, 92697-2025, USA
[4] Atmospheric Chemistry Department, Max Planck Institute for Chemistry, 55128 Mainz, Germany
[5] National Observatory of Athens, Institute for Environmental Research & Sustainable Development, 15236 Palea Penteli, Greece
[6] Forschungszentrum Jülich, Institute of Energy & Climate Research, IEK-8, D-52425 Jülich, Germany
[7] The Cyprus Institute, Nicosia 1645, Cyprus
[a] Now at: Chemical Science Division, Lawrence Berkeley National Laboratory, Berkeley, California, 94611, USA

Correspondence to: Allan Bertram (bertram@chem.ubc.ca)

Abstract. Information on the rate of diffusion of organic molecules within secondary organic aerosol (SOA) is needed to accurately predict the effects of SOA on climate and air quality. ~~These differences~~Diffusion can be important for predicting growth, evaporation, and reaction rates of SOA under certain atmospheric conditions.~~in the middle and upper part of the troposphere.~~ Often, researchers have predicted diffusion rates of organic molecules within SOA using measurements of viscosity and the Stokes-Einstein relation ($D \propto 1/\eta$ where D is the diffusion coefficient and η is viscosity). However, the accuracy of this relation for predicting diffusion in SOA remains uncertain. Using rectangular area fluorescence recovery after photobleaching (rFRAP), ~~W~~we determined~~measured~~ diffusion coefficients of fluorescent organic molecules over eight orders in magnitude in proxies of SOA including citric acid, sorbitol, and a sucrose-citric acid mixture. These results were combined with literature data to evaluate the Stokes-Einstein relation for predicting diffusion of organic molecules in SOA. Although almost all the data agrees with the Stokes-Einstein relation within a factor of ten, a fractional Stokes-Einstein relation ($D \propto$ ~~C~~$1/\eta^{\xi}$) with ~~ξ~~ ξ = 0.93~~ and C = 1.66~~ is a better model for predicting diffusion of organic molecules in the SOA proxies studied. In addition, based on the output from a chemical transport model, the Stokes-Einstein relation can over predict mixing times of organic molecules within SOA by as much as one order of magnitude at an altitude ~3 km, compared to the fractional Stokes-Einstein relation with ~~ξ~~ ξ = 0.93~~ and C = 1.66~~. ~~These differences can be important for predicting growth, evaporation, and reaction rates of SOA in the middle and upper part of the troposphere.~~ These results also have implications for other areas such as in food sciences and the preservation of biomolecules.~~where diffusion of organic molecules within organic water matrices is important.~~

1 Introduction

Atmospheric aerosols, suspensions of micrometer and sub-micrometer particles in the Earth's atmosphere, modify climate by interacting with incoming solar radiation and by altering cloud formation and cloud properties (Stocker et al., 2013). These aerosols also negatively impact air quality and may facilitate the long-range transport of pollutants (Friedman et al., 2014; Mu et al., 2018; Shrivastava et al., 2017a; Vaden et al., 2011; Zelenyuk et al., 2012).

A large fraction of atmospheric aerosols are classified as secondary organic aerosol (SOA). SOA is formed in the atmosphere when volatile organic molecules, emitted from both anthropogenic and natural sources, are oxidized and partition to the particle phase (Ervens et al., 2011; Hallquist et al., 2009). The exact chemical composition of SOA remains uncertain; however, measurements have shown that SOA contains 1000s of different organic molecules and the average oxygen-to-carbon (O:C) ratio of organic molecules in SOA ranges from 0.3 – 1.0 or even higher (Aiken et al., 2008; Cappa and Wilson, 2012; Chen et al., 2009; DeCarlo et al., 2008; Ditto et al., 2018; Hawkins et al., 2010; Heald et al., 2010; Jimenez et al., 2009; Laskin et al., 2018; Ng et al., 2010; Nozière et al., 2015; Takahama et al., 2011; Tsimpidi et al., 2018). SOA also contains a range of organic functional groups including alcohols and carboxylic acids (Claeys et al., 2004, 2007; Edney et al., 2005; Fisseha et al., 2004; Glasius et al., 2000; Liu et al., 2011; Surratt et al., 2006, 2010).

In order to accurately predict the impacts of SOA on climate, air quality, and the long-range transport of pollutants, information on the rate of diffusion of organic molecules within SOA is needed. For example, ~~predictions of SOA mass, which has major implications for climate and air quality, can vary by an order of magnitude when the molecular diffusion rate of organic molecules in SOA is varied in models (Shiraiwa and Seinfeld, 2012). P~~predictions of SOA particle size, which has implications for climate and visibility, ~~also~~ varies significantly in simulations as the diffusion rate of organic molecules is varied from 10^{-17} to 10^{-19} m^2 s^{-1} (Zaveri et al., 2014~~, 2018~~). Lifetimes of polyaromatic hydrocarbons (PAHs) in an SOA particle increase as the bulk diffusion coefficient of PAHs decreases from 10^{-16} m^2 s^{-1} at a relative humidity of 50% to 10^{-18} m^2 s^{-1} under dry conditions (Zhou et al., 2019). Shrivastava et al. (2017a) have shown that including shielding by a viscous organic aerosol coating (equivalent to a bulk diffusion limitation) results in better model predictions of observed concentrations of PAHs. Reactivity ~~and photochemistry~~ in SOA can also depend on diffusion rates of organic molecules (Davies and Wilson, 2015; ~~Hinks et al., 2016;~~ Lakey et al., 2016; Li et al., 2015; ~~Lignell et al., 2014;~~ Liu et al., 2018; Shiraiwa et al., 2011; Zhang et al., 2018; Zhou et al., 2013). For the cases discussed above, diffusion of organic molecules within SOA becomes a rate-limiting step only when diffusion rates are small.

In some cases, diffusion rates of organic molecules in SOA have been measured or inferred from experiments (Abramson et al., 2013; Liu et al., 2016; Perraud et al., 2012; Ullmann et al., 2019; Ye et al., 2016). However, in most cases researchers have predicted diffusion rates of organic molecules within SOA using measurements of viscosities and the Stokes-Einstein relation (Booth et al., 2014; Hosny et al., 2013; Koop et al., 2011; Maclean et al., 2017; Power et al., 2013; Renbaum-Wolff et al., 2013; Shiraiwa et al., 2011; Song et al., 2015, 2016a). This is due to the development and application of several techniques which can measure viscosity of ambient aerosol or small volumes in the laboratory (Grayson et al., 2015; Pajunoja et al., 2014;

Renbaum-Wolff et al., 2013; Song et al., 2016b; Virtanen et al., 2010). The Stokes-Einstein relation (Eq. 1) states that diffusion is inversely related to viscosity:

$$D = \frac{kT}{6\pi\eta R_H} \quad (1)$$

where D is the diffusion coefficient, k is the Boltzmann constant, T is the temperature in Kelvin, R_H is the hydrodynamic radius of the diffusing species, and η is the viscosity of the matrix. Until now, only a few studies have investigated the accuracy of the Stokes-Einstein relation for predicting diffusion coefficients of organic molecules in SOA, and almost all of these studies relied on sucrose as a proxy for SOA particles (Bastelberger et al., 2017; Chenyakin et al., 2017; Price et al., 2016). Sucrose was used as a proxy for SOA in these studies because 1) sucrose has an O:C ratio similar to that of highly oxidized components of SOA and 2) viscosity and diffusion data for sucrose exist~~ed~~ in the literature (mainly from the food science literature, as well as from Power et al. (2013), who reported viscosities far outside the range of what had previously been reported). However, studies with other proxies of SOA are required to determine if the Stokes-Einstein relation can accurately represent the diffusion of organic molecules in SOA, and to more accurately predict the role of SOA in climate, air quality, and transport of pollutants (Reid et al., 2018; Shrivastava et al., 2017b).

In the following, we expand on the previous studies with sucrose matrices by testing the Stokes-Einstein relation in the following proxies for SOA: 2-hydroxypropane-1,2,3-tricarboxylic acid (i.e. citric acid), 1,2,3,4,5,6-hexanol (i.e. sorbitol), and a mixture of citric acid and sucrose. These proxies have functional groups that have been identified in SOA, and O:C ratios similar to those ratios found in the most highly oxidized components of SOA in the atmosphere (1.16, 1.0, and 0.92 for citric acid, sorbitol, and sucrose respectively). To test the Stokes-Einstein relation, we first determined diffusion coefficients of fluorescent organic molecules as a function of water activity (a_w) in these SOA proxies using rectangular area fluorescence recovery after photobleaching (rFRAP; Deschout et al., 2010). Studies as a function of a_w are critical because as the relative humidity (RH) changes in the atmosphere, a_w (and hence water content) in SOA will change to maintain equilibrium with the gas phase. The diffusing organic molecules studied in this work were the fluorescent organic molecules rhodamine 6G and cresyl violet (Fig. S1). Details of the experiments are given in the Methods section. The ~~measured~~experimental diffusion coefficients are compared with predictions using literature viscosities (Rovelli et al., 2019; Song et al., 2016b) and the Stokes-Einstein relation. The results from the current study are then combined with literature diffusion (Champion et al., 1997; Chenyakin et al., 2017; Price et al., 2016; Rampp et al., 2000; Ullmann et al., 2019) and viscosity (Först et al., 2002; Grayson et al., 2017; Green and Perry, 2007; Haynes, 2015; Lide, 2001; Migliori et al., 2007; Power et al., 2013; Quintas et al., 2006; Rovelli et al., 2019; Swindells et al., 1958; Telis et al., 2007; Ullmann et al., 2019) data to assess the ability of the Stokes-Einstein relation to predict diffusion of organic molecules in atmospheric SOA. The ability of the fractional Stokes-Einstein relation (see below) to predict diffusion is also tested.

In addition to atmospheric applications, the results from this study have implications for other areas where diffusion of organic molecules within organic-water matrices is important, such as the cryopreservation of proteins (Cicerone and Douglas, 2012; Fox, 1995; Miller et al., 1998), the storage of food products (Champion et al., 1997; van der Sman and Meinders, 2013), and the viability of pharmaceutical formulations (Shamblin et al., 1999). The results also have implications for our understanding of the properties of deeply supercooled and supersaturated glass forming solutions, which are important for a wide range of applications and technologies (Angell, 1995; Debenedetti and Stillinger, 2001; Ediger, 2000).

2 Methods

2.1 Preparation of fluorescent organic-water films

The technique used here to determine~~measure~~ diffusion coefficients required thin films containing the organic matrix (i.e. citric acid or sorbitol or a mixture of citric acid and sucrose), water, and trace amounts of the diffusing organic molecules (i.e. fluorescent organic molecules). Citric acid (≥ 99 % purity) and sorbitol (≥ 98 % purity) were purchased from Sigma-Aldrich and used as received. Rhodamine 6G chloride (≥ 99 % purity), and cresyl violet acetate (≥75 % purity) were purchased from Acros Organics and Santa Cruz Biotechnology respectively, and used as received. Solutions containing the organic matrix, water, and the diffusing molecules were prepared gravimetrically. 55 weight percent citric acid solutions and 30 weight percent sorbitol and sucrose-citric acid solutions were used to prepare the citric acid, sorbitol, and sucrose-citric acid thin films, respectively. A mass ratio of 60:40 sucrose to citric acid was used for the sucrose-citric acid matrix. The concentrations of rhodamine 6G and cresyl violet in the solutions were 0.06 mM and 0.08 mM, respectively. After the solutions were prepared gravimetrically, the solutions were passed through a 0.02 µm filter (Whatman™) to eliminate impurities. Droplets of the solution were placed on cleaned siliconized hydrophobic slides (Hampton Research), by either nebulizing the bulk solution or using the tip of a sterilized needle (BD PrecisionGlide Needle, BD, Franklin Lakes, NJ, USA). The generated droplets ranged in diameter from ~100 to ~1300 µm. After the droplets were located on the hydrophobic slides, the hydrophobic slides were placed inside sealed glass containers with a controlled water activity (a_w). The a_w was set by placing saturated inorganic salt solutions with known a_w values within the sealed glass containers. The a_w values used ranged from 0.14 to 0.86. When the a_w values were higher than 0.86 recovery times were too fast to measure with the rFRAP setup. When the a_w values were lower than 0.14 or 0.23, depending on the organic solute, solution droplets often crystallized. The slides holding the droplets were left inside the sealed glass containers for an extended period of time to allow the droplets to equilibrate with the surrounding a_w. The method used to calculate equilibration times is explained in Section S1, and conditioning times for all samples are given in Tables S1-S4. Experimental times for conditioning were a minimum of three times longer than calculated equilibration times.

After the droplets on the slides reached equilibrium with the a_w of the airspace over the salt solution, the sealed glass containers holding the slides and conditioned droplets were brought into a Glove Bag™ (Glas-Col). The a_w within the Glove Bag was controlled using a humidified flow of N_2 gas and monitored using a handheld hygrometer. The a_w within the Glove Bag™ was

set to the same a_w as used to condition the droplets, to prevent the droplets from being exposed to an unknown and uncontrolled a_w. To form a thin film, aluminum spacers were placed on the siliconized glass slide holding the droplets, followed by another siliconized glass slide, which sandwiched the droplets and the aluminum spacers. The thickness of the aluminum spacers (30-50 μm) determined the thickness of the thin film. The two slides were sealed together by vacuum grease spread around the perimeter of one slide before sandwiching (see Fig. S2 in the Supplement for details).

The organic matrices were often supersaturated with respect to crystalline citric acid or sorbitol. Nevertheless, crystallization was not observed in most cases until a_w values $\lesssim$ 0.14 - 0.23, depending on the organic matrix, because the solutions were passed through a 0.02 μm filter and the glass slides used to make the thin films were covered with a hydrophobic coating. Filtration likely removed heterogeneous nuclei that could initiate crystallization and the hydrophobic coating reduced the ability of these surfaces to promote heterogeneous nucleation (Bodsworth et al., 2010; Pant et al., 2006; Price et al., 2014; Wheeler and Bertram, 2012). In the cases where crystallization was observed, determined using optical microscopy, the films were not used in rFRAP experiments. An image demonstrating the difference in appearance between crystallized and non-crystallized droplets is given in Figure S3. We did not condition droplets without fluorescent organic molecules to determine the effect of the tracer molecules on crystallization. However, previous studies have shown that droplets with the compositions and range of a_w values studied here can exist in the metastable liquid state if heterogeneous nucleation by surfaces is reduced. Furthermore, since the concentration of the tracers in the droplets were so low, the tracers are not expected to change the driving force for crystallization in the droplets.

2.2 Rectangular area fluorescence recovery after photobleaching (rFRAP) technique and extraction of diffusion coefficients

Diffusion coefficients were determined~~measured~~ using the rFRAP technique reported by Deschout et al. (2010). The technique uses a confocal laser scanning microscope to photobleach fluorescent molecules in a specified volume of an organic thin film containing fluorescent molecules. The photobleaching event initially reduces the fluorescence intensity within the bleached volume. Afterward, the fluorescence intensity within the photobleached volume recovers due to the diffusion of fluorescent molecules from outside of the bleached region. From the time-dependent recovery of the fluorescence intensity, diffusion coefficients are determined. All diffusion experiments~~coefficients reported~~ here were performed~~measured~~ at 295 ± 1 K.

The rFRAP experiments were performed on a Zeiss Axio Observer LSM 510MP laser scanning microscope with a 10X, 0.3 NA objective and a pinhole setting between 80 and 120 μm. Photobleaching and the subsequent acquisition of recovery images were done using a 543 nm helium–neon (HeNe) laser. The bleach parameters (e.g. laser intensity, iterations, laser speed) were varied for each experiment so that the fraction of fluorescent molecules being photobleached in the bleach region was about 30%. A photobleaching of about 30% was suggested by Deschout et al. (2010), who report that diffusion coefficients determined using~~measured with~~ the rFRAP technique are independent of the extent of photobleaching up to a bleach depth of 50%. The energy absorbed by the thin film during photobleaching is not expected to affect experimental diffusion coefficients.

Although local heating may occur during photobleaching, the thermal diffusivity in the samples is orders of magnitude greater than the molecular diffusivity, and the heat resulting from photobleaching will dissipate to the surroundings on a timescale much faster than the diffusion of molecules will occur (Chenyakin et al., 2017). Measurements as a function of photobleaching size and power are consistent with this expectation (Chenyakin et al., 2017; Ullmann et al., 2019).

Bleached areas ranged from 20 μm^2 to 400 μm^2. The geometry of the photobleached region was a square with sides of length l_x and l_y ranging from 4.5 to 20 μm. Smaller bleach areas were used in experiments where diffusion was slower in order to shorten recovery times. Chenyakin et al. (2017) showed that experimental~~measured~~ diffusion coefficients varied by less than the experimental uncertainty when the bleach area was varied from 1 μm^2 to 2500 μm^2 in sucrose-water films. Similarly, Deschout et al. (2010) demonstrated that diffusion coefficients varied by less than the experimental uncertainty when the bleach area was varied from approximately 4 μm^2 to 144 μm^2 in sucrose-water films. The images collected during a rFRAP experiment represent fluorescence intensities as a function of x and y coordinates, and are taken at regular time intervals after photobleaching. An example of images recorded during a rFRAP experiment are shown in Fig. S4. Every image taken following the photobleaching event is normalized relative to an image taken before photobleaching. To reduce noise, all images are downsized by averaging from a resolution of 512x512 pixels to 128x128 pixels.

The mathematical description of the fluorescence intensity as a function of position (x and y) and time (t) after photobleaching a rectangular area in a thin film, was given by Deschout et al. (2010):

$$\frac{F(x,y,t)}{F_0(x,y)} = \left[1 - \frac{K_0}{4} \cdot \left(\mathrm{erf}\left(\frac{x+\frac{l_x}{2}}{\sqrt{r^2+4Dt}}\right) - \mathrm{erf}\left(\frac{x-\frac{l_x}{2}}{\sqrt{r^2+4Dt}}\right)\right) \cdot \left(\mathrm{erf}\left(\frac{y+\frac{l_y}{2}}{\sqrt{r^2+4Dt}}\right) - \mathrm{erf}\left(\frac{y-\frac{l_y}{2}}{\sqrt{r^2+4Dt}}\right)\right)\right] \quad (2)$$

where $F(x,y,t)$ is the fluorescence intensity at position x and y after a time t, $F_0(x,y)$ corresponds to the initial intensity at position x and y before photobleaching, K_0 is related to the initial fraction of photobleached molecules in the bleach region, and l_x and l_y correspond to the size (length) of the bleach region in the x and y directions. The parameter r represents the resolution of the microscope, t is the time after photobleaching, and D is the diffusion coefficient.

The entire images (128x128 pixels following downsizing) collected during a rFRAP experiment were fit to Eq. (2) using a Matlab script (The Mathworks, Natick, MA, USA), with the terms K_0, and $r^2 + 4Dt$ left as free parameters. An additional normalization factor was also left as a free parameter, and returned a value close to 1, since images recorded after photobleaching were normalized to the pre-bleach image before fitting. To determine the bleach width (l_x, l_y), Eq. (2) was fit to the first five images recorded after photobleaching a film with the bleach width (l_x, l_y) left as a free parameter. The bleach width returned by the fit to the first five frames was then used as input in Eq. (2) to analyze the full set of images.

From the fitting procedure, a value for r^2+4Dt was determined for each image, and was plotted as a function of time after photobleaching. A straight line was then fit to the r^2+4Dt vs. t plot, and from the slope of the line D was calculated. An example is shown in Fig. S5. As the intensity of the fluorescence in the bleached region recovers, the noise in the data become large relative to the difference in fluorescence intensity between the bleached and non-bleached regions (i.e. signal). To ensure we

only use data with a reasonable signal to noise, images were not used if this signal was less than 3× the standard deviation of the noise.

Figure S6 shows a cross section of the fluorescence intensity along the x direction from the data in Fig. S4. Figure S6 is given only to visualize the fit of the equation to the data, and the cross-sectional fit was not used to determine diffusion coefficients. As mentioned above, the entire images (128x128 pixels following downsizing) were used to determine diffusion coefficients. To generate the cross-sectional view, at each position x, the measured fluorescence intensity is averaged over the width of the photobleached region in the y direction (black squares). Also included in Fig. S6 are cross-sectional views of the calculated fluorescence intensity along the x direction generated from the fitting procedure (solid red lines). To generate the line, Eq. (2) was first fit to the images. The resulting fit was then averaged over the width of the photobleached region in the y direction. The good agreement between the measured cross section and the predicted cross section illustrates that Eq. (2) describes the rFRAP data well.

Equation (2) assumes that there is no net diffusion in the axial direction (i.e. z-direction). Deschout et al. (2010) have shown that Eq. (2) gives accurate diffusion coefficients when the numerical aperture of the microscope is low (≤ 0.45) and the thickness of the fluorescent films is small (≤ 120 μm), which is consistent with the numerical aperture of 0.30 and film thickness of 30–50 μm used here.

3 Results and Discussion

3.1 Diffusion coefficients of organic molecules in citric acid, sorbitol, and sucrose-citric acid matrices

The ~~measured~~ experimental diffusion coefficients of organic molecules in matrices of citric acid, sorbitol, and sucrose-citric acid as a function of water activity (a_w) are shown in Fig. 1 (and listed in Tables S1-S4). The experimental~~measured~~ diffusion coefficients depend strongly on a_w for all three proxies of SOA. As a_w increases from 0.23 (0.14 in one case) to 0.86, diffusion coefficients increase by between five and eight orders of magnitude. This dependence on a_w arises from the plasticizing influence of water on these matrices; as a_w increases (and hence the water content increases) the viscosity decreases (Koop et al., 2011). In addition, the ~~measured~~ experimental diffusion coefficients varied significantly from matrix to matrix at the same a_w (Fig. 1). As an example, at $a_w = 0.23$ the diffusion coefficient of rhodamine 6G is about four orders of magnitude larger in citric acid compared to the sucrose-citric acid mixture.

We also considered the relationship between log (D) – log ($kT/6\pi R_H$) and log (η), a comparison that allows the identification of deviations from the Stokes-Einstein relation (Fig. 2). By plotting log (D) – log ($kT/6\pi R_H$), we account for differences in hydrodynamic radii of diffusing species and small differences in temperature (within a range of 6 K). The viscosity corresponding to each ~~measured~~ diffusion coefficient was determined from relationships between a_w and viscosity developed from literature data (Figs. S7-S9). The solid line in Fig. 2 corresponds to the relationship between log (D) – log ($kT/6\pi R_H$) and log (η) if the Stokes-Einstein relation (Eq. 1) is obeyed. Figure 2 shows that the diffusion coefficients of the fluorescent organic molecules depend strongly on viscosity, with the diffusion coefficients varying by approximately eight orders of

magnitude as viscosity varied by eight orders of magnitude. If the uncertainties of the measurements are considered, all the data points except three (89 % of the data) are consistent with predictions from the Stokes-Einstein relation (meaning that the error bars on the measurements overlap with the solid line in Fig. 2) over eight orders of magnitude change in diffusion coefficients. This finding is remarkable considering the assumptions inherent in the Stokes-Einstein relation (e.g. the diffusing species is a hard sphere that experiences the fluid as a homogeneous continuum and no slip at the boundary of the diffusing species).

3.2 Comparison with relevant literature data

Previous studies have used sucrose to evaluate the ability of the Stokes-Einstein relation to predict diffusion coefficients of organic molecules in SOA (Bastelberger et al., 2017; Chenyakin et al., 2017; Price et al., 2016). In addition, a recent study (Ullmann et al., 2019) used SOA generated in the laboratory from the oxidation of limonene, subsequently exposed to $NH_{3\,(g)}$ (i.e. brown limonene SOA) to evaluate the Stokes-Einstein relation. Although studies with SOA generated in the laboratory are especially interesting, that previous study was limited to relatively low viscosities ($\leq 10^2$ Pa s), where a breakdown of the Stokes-Einstein relation is less expected. In Fig. 3a, we have combined the results from the current study (i.e. the results from Fig. 2) with previous studies of diffusion and viscosity in sucrose and brown limonene SOA (Champion et al., 1997; Chenyakin et al., 2017; Price et al., 2016; Rampp et al., 2000; Ullmann et al., 2019). To be consistent with the current study, we have not included data in Fig. 3a if the diffusion coefficients and viscosities were measured at, or calculated using, temperatures outside the range of 292 – 298 K and if the radius of the diffusing molecule was smaller than ~~to~~ the radius of the molecules in the fluid matrix. Previous work has shown that the Stokes-Einstein relation is not applicable when the radius of the diffusing molecule is less than the radius of the matrix molecules, and those cases are beyond the scope of this work (Bastelberger et al., 2017; Davies and Wilson, 2016; Marshall et al., 2016; Power et al., 2013; Price et al., 2016; Shiraiwa et al., 2011). Additional details for the data shown in Fig. 3a are included in section S2 and Table S5.

Based on Fig. 3a the diffusion coefficients of the organic molecules in sucrose matrices and matrices consisting of SOA generated in the laboratory depend strongly on viscosity, similar to the results shown in Fig. 2. In addition, almost all the data agree with the Stokes-Einstein relation (solid line in Fig. 3a) within a factor of ten. This finding is in stark contrast with the diffusion of water in organic-water mixtures, where much larger deviations between experimental~~measured~~ and predicted diffusion coefficients were observed over the same viscosity range (Davies and Wilson, 2016; Marshall et al., 2016; Price et al., 2016).

In Fig. 3b, we show the differences between the ~~measured~~experimental values and the solid line in Fig. 3a as a function of viscosity. If the Stokes-Einstein relation describes the data well, these differences (i.e. residuals) should be scattered symmetrically about zero, while the magnitude of the residuals should be less than or equal to the uncertainty in the measurements. However, the residuals are skewed to be positive, especially as viscosity increases, with experimental~~measured~~

diffusion faster than expected based on the Stokes-Einstein relation. Figure 3b suggests that the Stokes-Einstein relation may not be the optimal model for predicting diffusion coefficients in SOA, particularly at high viscosities.

3.3 Fractional Stokes-Einstein relation

When deviation from the Stokes-Einstein relation has been observed in the past, a fractional Stokes-Einstein relation ($D \propto 1/\eta^{\xi}$, where ξ is an empirical fit parameter) has often been used to quantify the relationship between diffusion and viscosity. For example, Price et al. (2016) showed that a fractional Stokes-Einstein relation can accurately represent the diffusion of sucrose in a sucrose matrix over a wide range of viscosities (from roughly $10^0 - 10^6$ Pa s) with $\xi = 0.90$. Building on that work, the data in Fig. 3a were fit to the following fractional Stokes-Einstein relation:

$$D = D_c \left(\frac{\eta_c}{\eta}\right)^{\xi} \quad (3)$$

where ξ is an empirical fit parameter, η_c is the crossover viscosity, and D_c is the crossover diffusion coefficient. The crossover viscosity is the viscosity at which the Stokes-Einstein relation and the fractional Stokes-Einstein relation predict the same diffusion coefficient. Based on the data in Fig. 3 we have chosen $\eta_c = 10^{-3}$ Pa s. The crossover diffusion coefficient corresponds to the diffusion coefficient at η_c (which can be calculated with the Stokes-Einstein relation). The value of ξ is determined as the slope of the dashed line in Fig. 3a. The best fit to the data (represented by the dashed line in Fig. 3a) resulted in a ξ value of 0.93. Each data point was weighted equally when performing the fitting.

In Fig. 3c, we plotted the difference between the experimental values shown in Fig. 3a and the predicted values using the fractional Stokes-Einstein relation (dashed line in Fig. 3a). These residuals are more symmetrically scattered about zero compared to the residuals plotted in Fig. 3b. In addition, the sum-of-squared residuals (r^2) in Fig 3c was less than the sum-of-squared residuals in Fig. 3b ($r^2 = 10.8$ compared to 19.7). Beyond the sum-of-squared residuals test we have performed a reduced chi-squared (χ^2) test which takes into account the extra fitting variable present in the fractional Stokes-Einstein relation. Assuming a variance of 0.25, the reduced χ^2 value is 1.24 for the Stokes-Einstein relation and is 0.67 for the fractional Stokes-Einstein relation. This information suggests that the fractional Stokes-Einstein relation with an exponent value of $\xi = 0.93$ may be the better model for predicting diffusion coefficients of organic molecules in SOA compared to the traditional Stokes-Einstein relation. This is in close agreement with the findings of Price et al. (2016) who showed that the diffusion of sucrose in a sucrose-water matrix could be modelled using a fractional Stokes-Einstein relation with $\xi = 0.90$ over a large range in viscosity. The new fractional Stokes-Einstein relation, which builds on the work of Price et al. (2016), was derived using diffusion data of several large organic molecules in several types of organic water-matrices, and thus demonstrates a broader utility of the fractional Stokes-Einstein relation.

For the case of large diffusing molecules such as those included in this work (i.e. the radius of the diffusing molecule is equal to or larger than the radius of the organic molecules in the matrix), we do not observe a strong dependence of ξ on the size or

nature of the diffusing molecule. For smaller molecules, ξ is expected to change significantly. For example, Price et al., (2016) showed that ξ = 0.57 for the diffusion of water in a sucrose-water matrix, and (Pollack (1981) showed that ξ = 0.63 for diffusion of xenon in a sucrose-water matrix. The development of a relationship between ξ and the size of small diffusing molecules is beyond the scope of this work.

3.4 Implications for atmospheric mixing times

To investigate the atmospheric implications of these results, we considered the mixing times of organic molecules within SOA in the atmosphere as a function of viscosity using both the Stokes-Einstein relation (Eq. 1) and the fractional Stokes-Einstein relation (Eq. 3) with t^{ξ} = 0.93 ~~and C = 1.66~~. Mixing times were calculated with the following equation (Seinfeld and Pandis, 2006; Shiraiwa et al., 2011):

$$\tau_{mix} = \frac{{d_p}^2}{4\pi^2 D} \quad (4)$$

where τ_{mix} is the characteristic mixing time, d_p is the SOA particle diameter, and D is the diffusion coefficient. τ_{mix} corresponds to the time at which the concentration of the diffusing molecules at the centre of the particle deviates by less than a factor of 1/e from the equilibrium concentration. We assumed a d_p of 200 nm, which is roughly the median diameter in the volume distribution of ambient SOA (Martin et al., 2010; Pöschl et al., 2010; Riipinen et al., 2011). We assumed a value of 0.38 nm for R_H based on literature values for molecular weight (175 g mol^{-1}; Huff Hartz et al., 2005) and the density (1.3 g cm^{-3}; Chen and Hopke, 2009; Saathoff et al., 2009) of SOA molecules, and assuming a spherical symmetry of the diffusing species.

Figure 4 shows the calculated mixing times of 200 nm particles as a function of the viscosity of the matrix. The mixing time of 1 hour is highlighted, since when calculating the growth and evaporation of SOA and the long-range transport of pollutants using chemical transport models, a mixing times of < 1 hour for organic molecules within SOA is often assumed (Hallquist et al., 2009). At a viscosity of 5 x 10^6 Pa s, the mixing time is > 1 hour based on the Stokes-Einstein relation, but remains < 1 hour based on the fractional Stokes-Einstein relation. Furthermore, at high viscosities > 5 x 10^6 Pa s, the mixing times predicted with the traditional Stokes-Einstein relation are at least a factor of 5 greater than those predicted with the fractional Stokes-Einstein relation.

Recently, Shiraiwa et al. (2017) estimated mixing times of organic molecules in SOA particles in the global atmosphere using the global chemistry climate model EMAC (Jöckel et al., 2006) and the organic module ORACLE (Tsimpidi et al., 2014). Glass transition temperatures of SOA compounds were predicted based on molar mass and the O:C ratio of SOA components, followed by predictions of viscosity. Diffusion coefficients and mixing times were predicted using the Stokes-Einstein relation. To further explore the implications of our results, we calculated mixing times of organic molecules in SOA globally using the same approach as Shiraiwa et al. (2017) and compared predictions using the Stokes-Einstein relation and predictions using the fractional Stokes-Einstein relation with t^{ξ} = 0.93 ~~and C = 1.66~~. Shown in Fig. 5 are results from these calculations. At all latitudes at the surface, the mixing times are well below the 1 hour often assumed in chemical transport models, regardless if the Stokes-Einstein relation or the fractional Stokes-Einstein relation is used (Fig. 5a). On the other hand, at an

altitude of approximately 1.4 km, the latitudes where the mixing times exceed 1 hr will depend on whether the Stokes-Einstein relation or fractional Stokes-Einstein relation is used (Fig. 5b). At an altitude of 3.2 km the mixing times are well above the 1-hour cut-off regardless of what relation is used, and the Stokes-Einstein relation can over predict mixing times of SOA particles by as much as one order of magnitude compared to the fractional Stokes-Einstein relation (Fig. 5c). A caveat is that the predictions at 3.2 km are based on viscosities higher than the viscosities studied in the current work. Hence, at 3.2 km the Stokes-Einstein and fractional Stokes-Einstein relations are being used outside the viscosity range tested here. Although experimentally challenging, additional studies are recommended to determine if the fractional Stokes-Einstein relation with ~~t~~ξ = 0.93 ~~and C = 1.66~~ is able to accurately predict diffusion coefficients of organic molecules in proxies of SOA at viscosities higher than investigated in the current study.

4 Summary and Conclusions

We report experimental~~measured~~ diffusion coefficients of fluorescent organic molecules in a variety of SOA proxies. The reported diffusion coefficients varied by about eight orders of magnitude as the water activity in the SOA proxies varied from 0.23 (0.14 in one case) to 0.86. By combining the new diffusion coefficients with literature data, we have shown that, in almost all cases, the Stokes-Einstein relation correctly predicts diffusion coefficients of organic molecules in SOA proxies within a factor of ten. This finding is in stark contrast with the diffusion of water in SOA proxies, where much larger deviations between experimental~~measured~~ and predicted diffusion coefficients have been observed over the same viscosity range. Even though the Stokes-Einstein relation correctly predicts diffusion of organic molecules in the majority of cases within a factor of ten, a sum-of-squared residuals analysis shows that a fractional Stokes-Einstein relation with an exponent of ~~t~~ξ = 0.93 ~~and C = 1.66~~ is a better model for predicting diffusion coefficients in SOA proxies, for the range of viscosities included in this study. This is consistent with earlier work that showed the fractional Stokes-Einstein relation is able to reproduce experimental~~measured~~ diffusion coefficients of sucrose in sucrose-water matrices. The fractional Stokes-Einstein relation predicts faster diffusion coefficients and therefore shorter mixing times of SOA particles in the atmosphere. At an altitude of ~3.2 km, the difference in mixing times predicted by the two relations is as much as one order of magnitude.

Authors contributions

EE performed the diffusion experiments~~measurements~~. AMM, YL, APT, VAK, JL, and MS provided calculations of mixing times as a function of altitude and latitude. GR and JPR provided viscosity data. SK provided assistance with the diffusion experiments~~measurements~~. EE and AKB conceived the study and wrote the manuscript. All authors contributed toward revising the manuscript. All authors read and approved the final manuscript.

Conflicts of interest

There are no conflicts of interest to declare.

Data availability

Underlying data and related material for this paper are located in the Supplement.

Acknowledgements

This work was funded by the Natural Sciences and Engineering Research Council of Canada. Diffusion ~~measurements~~experiments were performed in the LASIR facility at UBC, funded by the Canadian Foundation for Innovation. APT acknowledges support from a DFG individual grant program (project reference TS 335/2-1). GR and JPR gratefully acknowledge support from NERC through the award of grants NE/N013700/1 and NE/M004600/1. MS and YL acknowledge funding from the U.S. National Science Foundation (AGS-1654104) and the U.S. Department of Energy (DE-SC0018349).

Figures

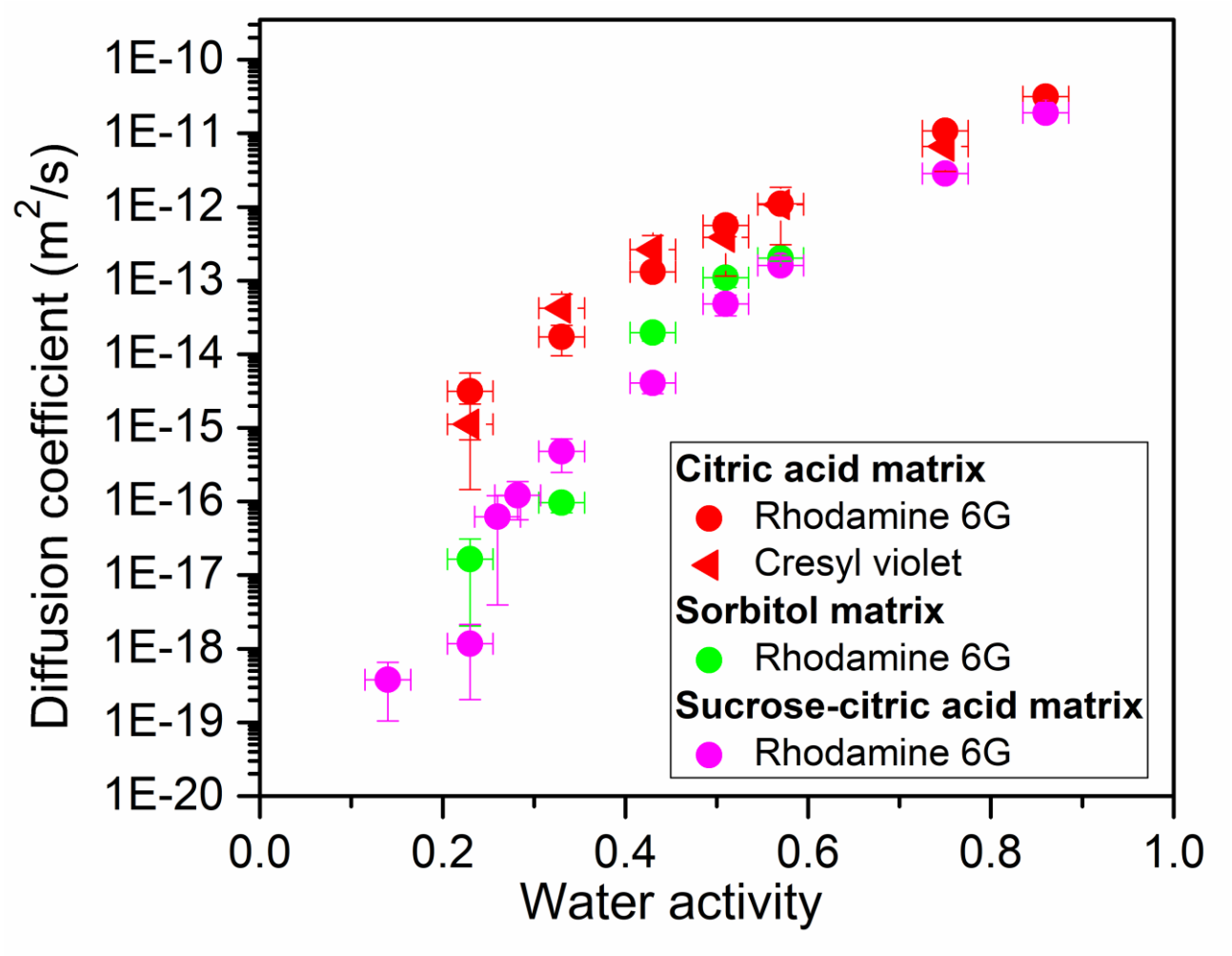

Figure 1. Experimental~~Measured~~ diffusion coefficients of fluorescent organic molecules in various organic matrices as a function of water activity (a_w). X-error bars represent the uncertainty in the measured a_w (± 0.025) and y-error bars correspond to two times the standard deviation in the diffusion measurements. Each data point is the average of a minimum of four measurements. Indicated in the legend are the fluorescent organic molecules studied and the corresponding matrices.

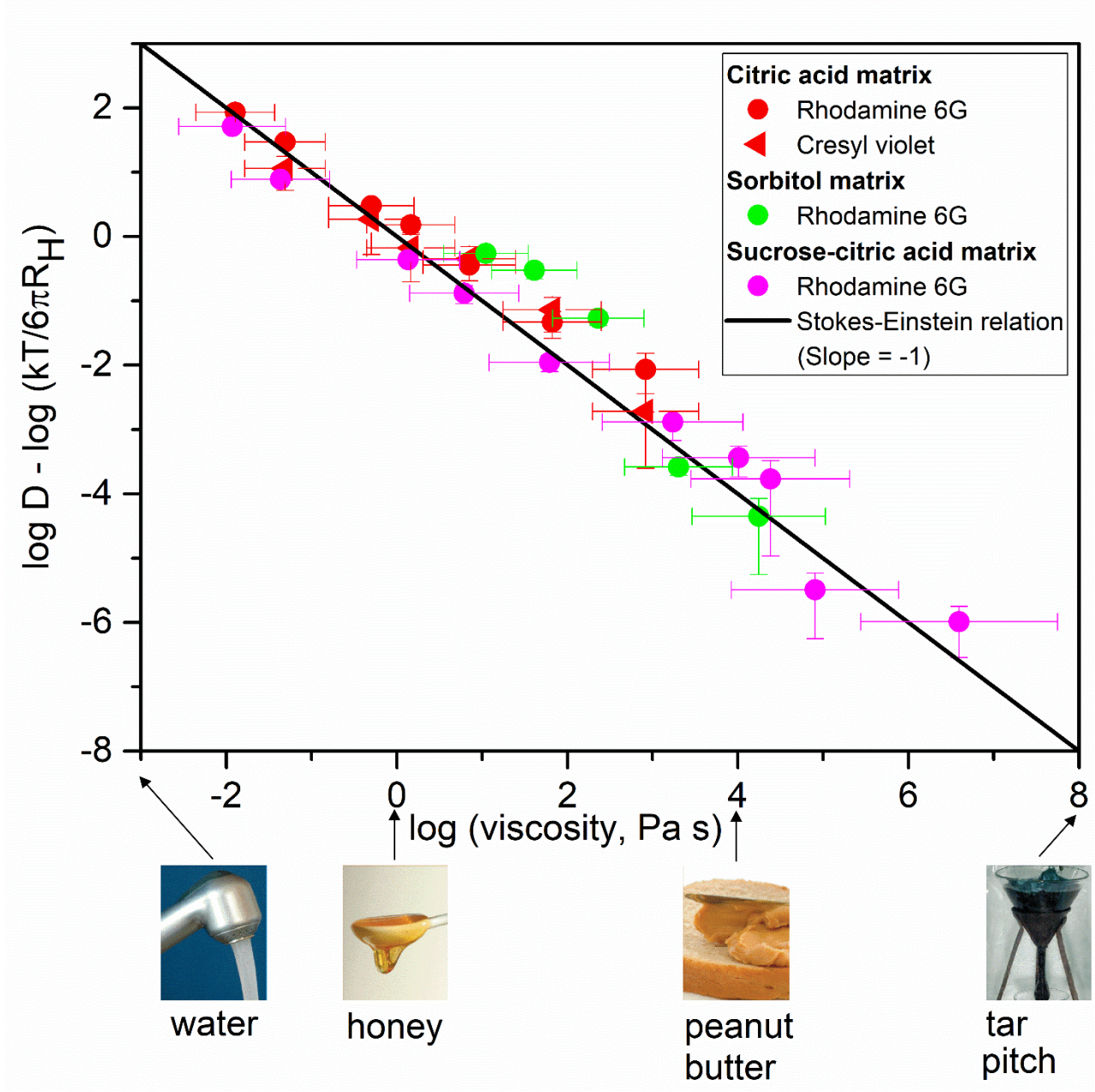

Figure 2. Plot of log (D) – log (kT/6πR$_H$) as a function of log (η) for ~~measurements~~diffusion coefficients shown in Fig. 1. Viscosities (η) were determined from relationships between viscosity and a_w (Figs. S7 –S9). T corresponds to the experimental temperature and R$_H$ corresponds to the radius of each diffusing species (see Table S5). The x-error bars were calculated using the uncertainty in a_w at which the samples were conditioned (± 0.025) and uncertainties in the viscosity-a_w parameterizations. The y-error bars represent ~~2~~ two times the standard deviation of the experimental diffusion coefficients~~measurements~~. The black line represents the relationship between log (D) – log (kT/6πR$_H$) and log (η) predicted by the Stokes-Einstein relation (slope = -1). Shown at the bottom of the figure are various substances and their approximate room temperature viscosities to provide context, as in Koop et al. (2011). The image of tar pitch is part of an image from the pitch drop experiment (image courtesy of Wikimedia Commons, GNU Free Documentation License, University of Queensland, John Mainstone).

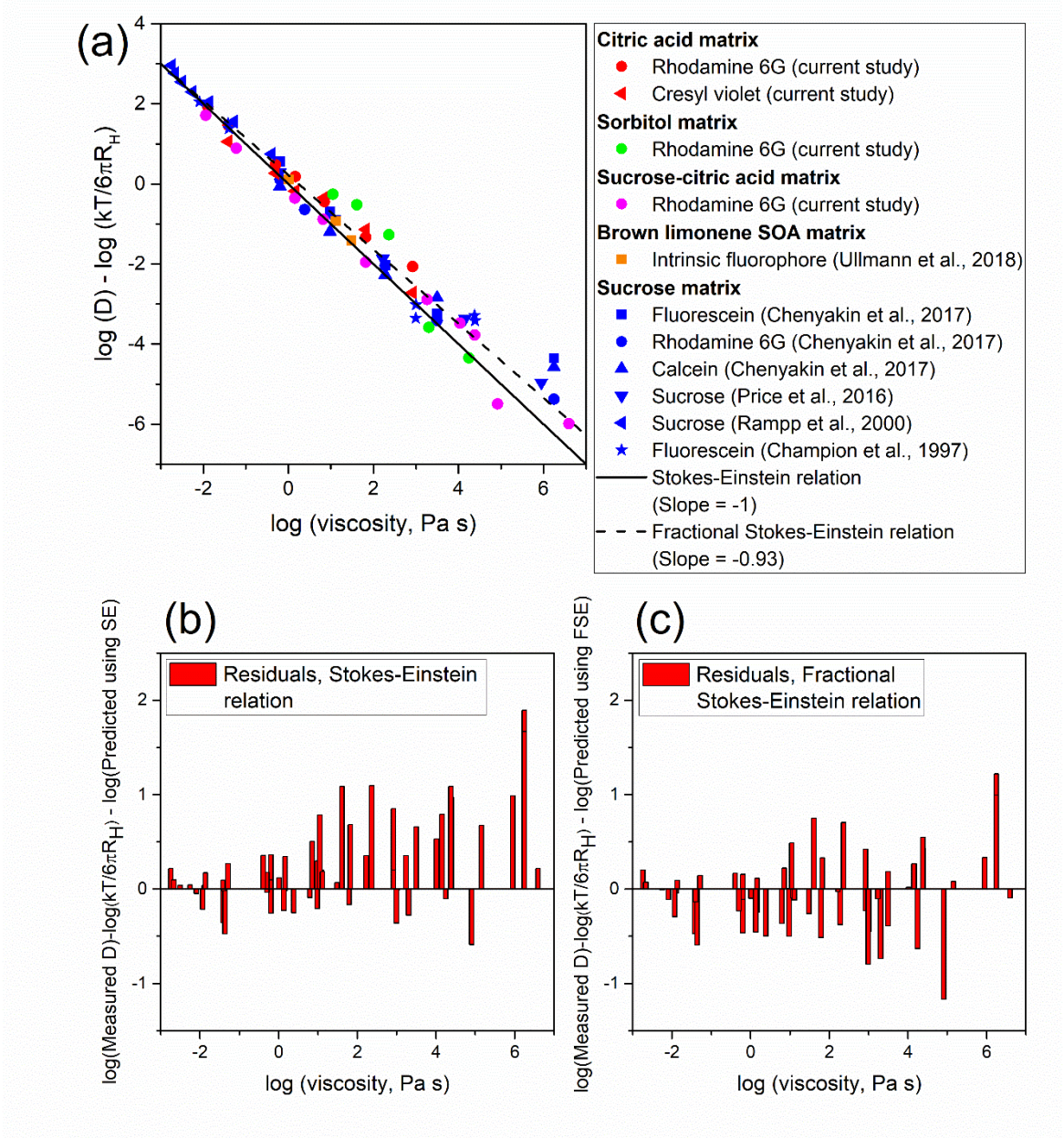

Figure 3. a) Plot of log (D) – log (kT/6πR$_H$) as a function of log (η) for ~~new measurements~~experimental diffusion coefficients reported in this work and literature data. Indicated in the legend are the diffusing organic molecules studied and the corresponding matrices. T corresponds to the experimental temperature of each diffusion coefficient ~~measurement~~ and R$_H$ corresponds to the radius of each diffusing species (Section S2 and Table S5). The symbols represent experimental~~measured~~ data points. The solid line represents the relationship between log (D) – log (kT/6πR$_H$) and log (η) predicted by the Stokes-Einstein relation, while the dashed line represents the relationship between log (D) – log (kT/6πR$_H$) and log (η) predicted by a fractional Stokes-Einstein relation with slope = -0.93 and crossover viscosity of 10^{-3} Pa s ~~and intercept 0.219 (equal to the log of the C value, 1.66)~~. Panels b) and c) are plots of the differences (i.e. residuals) between experimental~~measured~~ and predicted values of log (D) – log(kT/6πR$_H$) using the Stokes-Einstein relation and the fractional Stokes-Einstein relation, respectively. The sum-of-squared residuals for the Stokes-Einstein relation is 19.7 and the sum-of-squared residuals for the fractional Stokes-Einstein relation is 10.8.

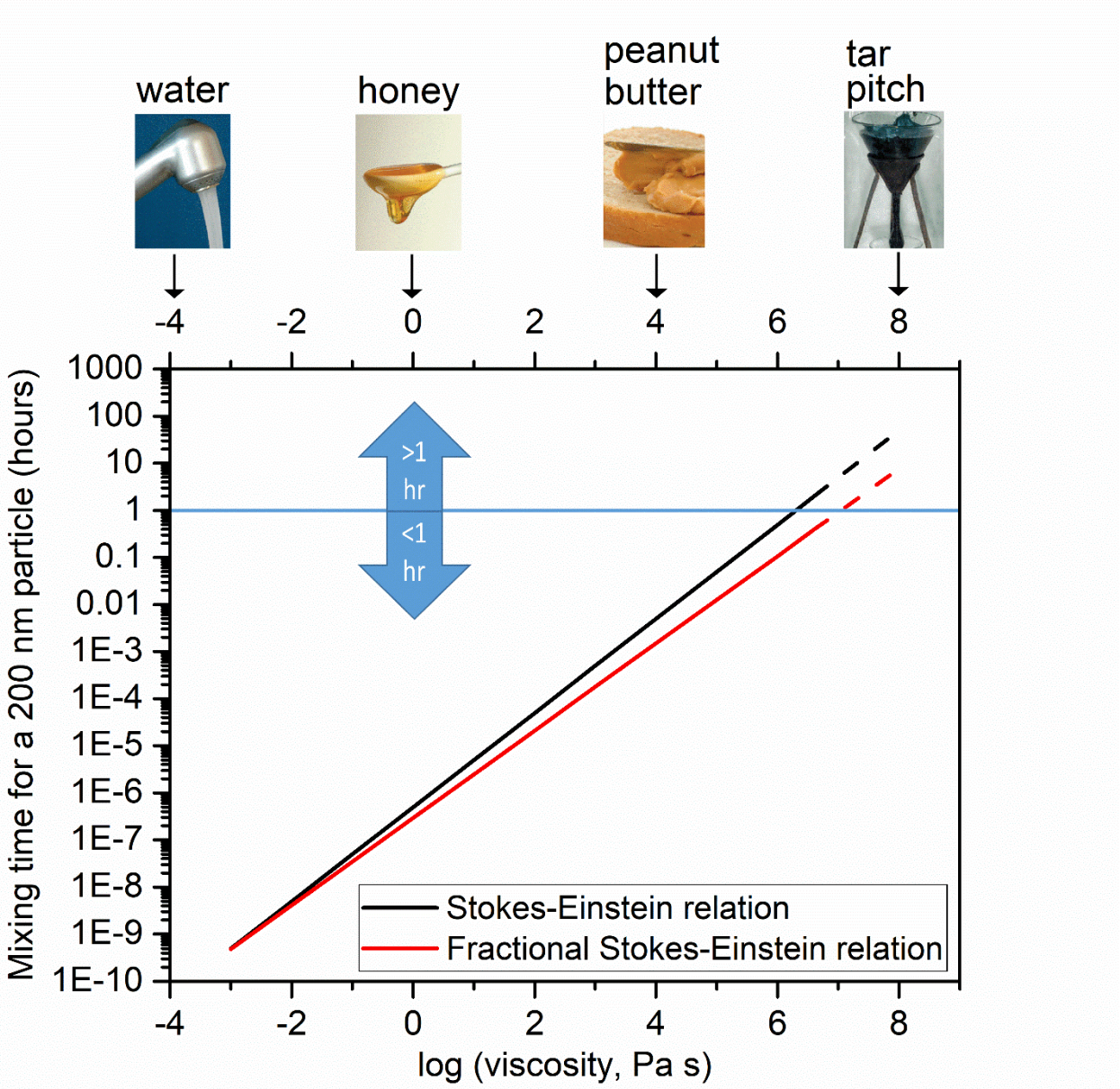

Figure 4. Mixing times of organic molecules within a 200 nm particle as a function of viscosity using the Stokes-Einstein relation (black line) and a fractional Stokes-Einstein relation (red line). The dashed lines indicate that the relations were extrapolated to viscosities beyond the tested range of viscosities (≥ 4 x 10^6 Pa s).

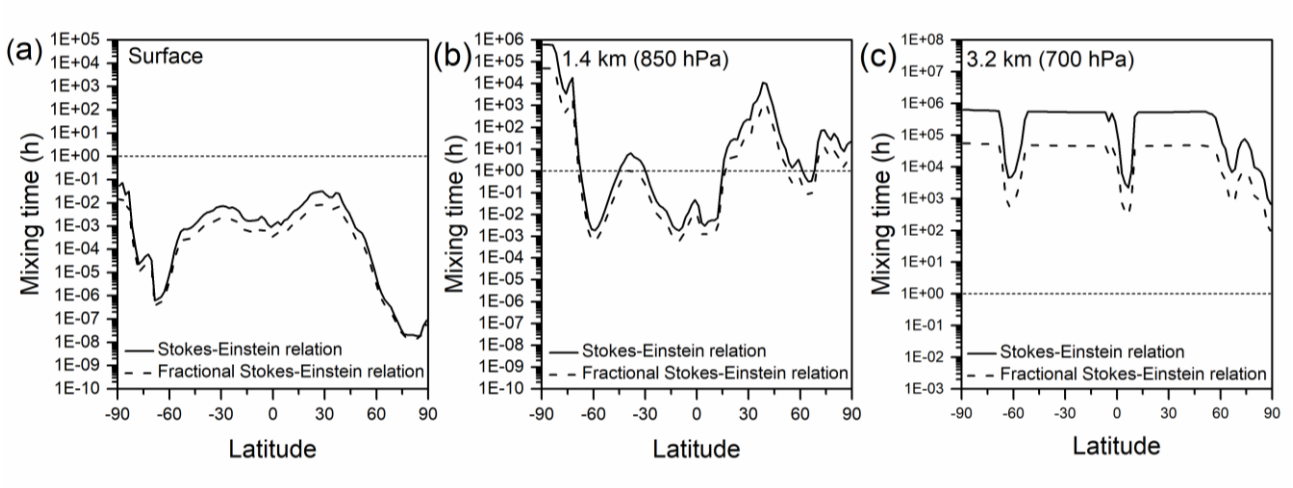

Figure 5. Mixing times (in hours) of organic molecules in 200 nm SOA particles at a) the surface, b) 850 hPa or ~1.4 km altitude, and c) 700 hPa or ~3.2 km altitude, using diffusion coefficients calculated with the Stokes-Einstein relation (solid black lines) and the fractional Stokes-Einstein relation (dashed black lines). A one-hour mixing time, which is often assumed in chemical transport models, is also indicated in each figure with a horizontal dotted line.

References

Abramson, E., Imre, D., Beránek, J., Wilson, J. and Zelenyuk, A.: Experimental determination of chemical diffusion within secondary organic aerosol particles., Phys. Chem. Chem. Phys., 15(8), 2983–2991, doi:10.1039/c2cp44013j, 2013.

Aiken, A. C., Decarlo, P. F., Kroll, J. H., Worsnop, D. R., Huffman, J. A., Docherty, K. S., Ulbrich, I. M., Mohr, C., Kimmel, J. R., Sueper, D., Sun, Y., Zhang, Q., Trimborn, A., Northway, M., Ziemann, P. J., Canagaratna, M. R., Onasch, T. B., Alfarra, M. R., Prevot, A. S. H., Dommen, J., Duplissy, J., Metzger, A., Baltensperger, U. and Jimenez, J. L.: O/C and OM/OC ratios of primary, secondary, and ambient organic aerosols with high-resolution time-of-flight aerosol mass spectrometry, Environ. Sci. Technol., 42(12), 4478–4485, doi:10.1021/es703009q, 2008.

Angell, C. A.: Formation of Glasses Fom Liquids and Biopolymers, Science (80-.)., 267(5206), 1924–1935, doi:10.1126/science.267.5206.1924, 1995.

Bastelberger, S., Krieger, U. K., Luo, B. and Peter, T.: Diffusivity measurements of volatile organics in levitated viscous aerosol particles, Atmos. Chem. Phys., 17(13), 8453–8471, doi:10.5194/acp-17-8453-2017, 2017.

Bodsworth, A., Zobrist, B. and Bertram, A. K.: Inhibition of efflorescence in mixed organic-inorganic particles at temperatures less than 250 K., Phys. Chem. Chem. Phys., 12(38), 12259–12266, doi:10.1039/c0cp00572j, 2010.

Booth, A. M., Murphy, B., Riipinen, I., Percival, C. J. and Topping, D. O.: Connecting bulk viscosity measurements to kinetic limitations on attaining equilibrium for a model aerosol composition, Environ. Sci. Technol., 48(16), 9298–9305, doi:10.1021/es501705c, 2014.

Cappa, C. D. and Wilson, K. R.: Multi-generation gas-phase oxidation, equilibrium partitioning, and the formation and

evolution of secondary organic aerosol, Atmos. Chem. Phys., 12(20), 9505–9528, doi:10.5194/acp-12-9505-2012, 2012.

Champion, D., Hervet, H., Blond, G., LeMeste, M. and Simatos, D.: Translational diffusion in sucrose solutions in the vicinity of their glass transition temperature, J. Phys. Chem. B., 101, 10674–10679, doi:10.1021/jp971899i, 1997.

Chen, Q., Farmer, D. K., Schneider, J., Zorn, S. R., Heald, C. L., Karl, T. G., Guenther, A., Allan, J. D., Robinson, N., Coe, H., Kimmel, J. R., Pauliquevis, T., Borrmann, S., Pöschl, U., Andreae, M. O., Artaxo, P., Jimenez, J. L. and Martin, S. T.: Mass spectral characterization of submicron biogenic organic particles in the Amazon Basin, Geophys. Res. Lett., 36(20), L20806, doi:10.1029/2009GL039880, 2009.

Chen, X. and Hopke, P. K.: Secondary organic aerosol from α-pinene ozonolysis in dynamic chamber system, Indoor Air, 19(4), 335–345, doi:10.1111/j.1600-0668.2009.00596.x, 2009.

Chenyakin, Y., Ullmann, D. A., Evoy, E., Renbaum-Wolff, L., Kamal, S. and Bertram, A. K.: Diffusion coefficients of organic molecules in sucrose-water solutions and comparison with Stokes-Einstein predictions, Atmos. Chem. Phys., 17, 2423–2435, doi:10.5194/acp-17-2423-2017, 2017.

Cicerone, M. T. and Douglas, J. F.: Beta-Relaxation governs protein stability in sugar-glass matrices, Soft Matter, 8, 2983–2991, doi:10.1039/c2sm06979b, 2012.

Claeys, M., Graham, B., Vas, G., Wang, W., Vermeylen, R., Pashynska, V., Cafmeyer, J., Guyon, P., Andreae, M. O., Artaxo, P. and Maenhaut, W.: Formation of secondary organic aerosols through photooxidation of isoprene, Science (80-.)., 303(5661), 1173–1176, doi:10.1126/science.1092805, 2004.

Claeys, M., Szmigielski, R., Kourtchev, I., Van Der Veken, P., Vermeylen, R., Maenhaut, W., Jaoui, M., Kleindienst, T. E., Lewandowski, M., Offenberg, J. H. and Edney, E. O.: Hydroxydicarboxylic acids: Markers for secondary organic aerosol from the photooxidation of α-pinene, Environ. Sci. Technol., 41(5), 1628–1634, doi:10.1021/es0620181, 2007.

Davies, J. F. and Wilson, K. R.: Nanoscale interfacial gradients formed by the reactive uptake of OH radicals onto viscous aerosol surfaces, Chem. Sci., 6(12), 7020–7027, doi:10.1039/c5sc02326b, 2015.

Davies, J. F. and Wilson, K. R.: Raman Spectroscopy of Isotopic Water Diffusion in Ultraviscous, Glassy, and Gel States in Aerosol by Use of Optical Tweezers, Anal. Chem., 88(4), 2361–2366, doi:10.1021/acs.analchem.5b04315, 2016.

Debenedetti, P. G. and Stillinger, F. H.: Supercooled liquids and the glass transition, Nature, 410, 259–267, doi:10.1038/35065704, 2001.

DeCarlo, P. F., Dunlea, E. J., Kimmel, J. R., Aiken, A. C., Sueper, D., Crounse, J., Wennberg, P. O., Emmons, L., Shinozuka, Y., Clarke, A., Zhou, J., Tomlinson, J., Collins, D. R., Knapp, D., Weinheimer, A. J., Montzka, D. D., Campos, T. and Jimenez, J. L.: Fast airborne aerosol size and chemistry measurements above Mexico City and Central Mexico during the MILAGRO campaign, Atmos. Chem. Phys., 8(14), 4027–4048, doi:10.5194/acp-8-4027-2008, 2008.

Deschout, H., Hagman, J., Fransson, S., Jonasson, J., Rudemo, M., Lorén, N. and Braeckmans, K.: Straightforward FRAP for quantitative diffusion measurements with a laser scanning microscope., Opt. Express, 18(22), 22886–22905, doi:10.1364/OE.18.022886, 2010.

Ditto, J. C., Barnes, E. B., Khare, P., Takeuchi, M., Joo, T., Bui, A. A. T., Lee-Taylor, J., Eris, G., Chen, Y., Aumont, B.,

Jimenez, J. L., Ng, N. L., Griffin, R. J. and Gentner, D. R.: An omnipresent diversity and variability in the chemical composition of atmospheric functionalized organic aerosol, Commun. Chem., 1(1), 75, doi:10.1038/s42004-018-0074-3, 2018.

Ediger, M. D.: Spatially Heterogeneous Dynamics in Supercooled Liquids, Annu. Rev. Phys. Chem., 51, 99–128, doi:10.1146/annurev.physchem.51.1.99, 2000.

Edney, E. O., Kleindienst, T. E., Jaoui, M., Lewandowski, M., Offenberg, J. H., Wang, W. and Claeys, M.: Formation of 2-methyl tetrols and 2-methylglyceric acid in secondary organic aerosol from laboratory irradiated isoprene/NOX/SO2/air mixtures and their detection in ambient PM2.5 samples collected in the eastern United States, Atmos. Environ., 39(29), 5281–5289, doi:10.1016/j.atmosenv.2005.05.031, 2005.

Ervens, B., Turpin, B. J. and Weber, R. J.: Secondary organic aerosol formation in cloud droplets and aqueous particles (aqSOA): A review of laboratory, field and model studies, Atmos. Chem. Phys., 11(21), 11069–11102, doi:10.5194/acp-11-11069-2011, 2011.

Fisseha, R., Dommen, J., Sax, M., Paulsen, D., Kalberer, M., Maurer, R., Höfler, F., Weingartner, E. and Baltensperger, U.: Identification of organic acids in secondary organic aerosol and the corresponding gas phase from chamber experiments, Anal. Chem., 76(22), 6535–6540, doi:10.1021/ac048975f, 2004.

Först, P., Werner, F. and Delgado, A.: On the pressure dependence of the viscosity of aqueous sugar solutions, Rheol. Acta, 41(4), 369–374, doi:10.1007/s00397-002-0238-y, 2002.

Fox, K. C.: Putting Proteins Under Glass, Science (80-.)., 267(5206), 1922–1923, doi:10.1126/science.7701317, 1995.

Friedman, C. L., Pierce, J. R. and Selin, N. E.: Assessing the influence of secondary organic versus primary carbonaceous aerosols on long-range atmospheric polycyclic aromatic hydrocarbon transport, Environ. Sci. Technol., 48(6), 3293–3302, doi:10.1021/es405219r, 2014.

Glasius, M., Lahaniati, M., Calogirou, A., Di Bella, D., Jensen, N. R., Hjorth, J., Kotzias, D. and Larsen, B. R.: Carboxylic acids in secondary aerosols from oxidation of cyclic monoterpenes by ozone, Environ. Sci. Technol., 34(6), 1001–1010, doi:10.1021/es990445r, 2000.

Grayson, J. W., Song, M., Sellier, M. and Bertram, A. K.: Validation of the poke-flow technique combined with simulations of fluid flow for determining viscosities in samples with small volumes and high viscosities, Atmos. Meas. Tech., 8(6), 2463–2472, doi:10.5194/amt-8-2463-2015, 2015.

Grayson, J. W., Evoy, E., Song, M., Chu, Y., Maclean, A., Nguyen, A., Upshur, M. A., Ebrahimi, M., Chan, C. K., Geiger, F. M., Thomson, R. J. and Bertram, A. K.: The effect of hydroxyl functional groups and molar mass on the viscosity of non-crystalline organic and organic-water particles, Atmos. Chem. Phys., 17(13), 8509–8524, doi:10.5194/acp-17-8509-2017, 2017.

Green, D. W. and Perry, R. H.: Perry's Chemical Engineers' Handbook, 8th ed., The McGraw-Hill Companies, New York, NY., 2007.

Hallquist, M., Wenger, J. C., Baltensperger, U., Rudich, Y., Simpson, D., Claeys, M., Dommen, J., Donahue, N. M., George, C., Goldstein, a. H., Hamilton, J. F., Herrmann, H., Hoffmann, T., Iinuma, Y., Jang, M., Jenkin, M. E., Jimenez, J. L., Kiendler-

Scharr, A., Maenhaut, W., McFiggans, G., Mentel, T. F., Monod, A., Prévôt, a. S. H., Seinfeld, J. H., Surratt, J. D., Szmigielski, R. and Wildt, J.: The formation, properties and impact of secondary organic aerosol: current and emerging issues, Atmos. Chem. Phys., 9(14), 5155–5236, doi:10.5194/acp-9-5155-2009, 2009.

Hawkins, L. N., Russell, L. M., Covert, D. S., Quinn, P. K. and Bates, T. S.: Carboxylic acids, sulfates, and organosulfates in processed continental organic aerosol over the southeast Pacific Ocean during VOCALS-REx 2008, J. Geophys. Res., 115, D13201, doi:10.1029/2009JD013276, 2010.

Haynes, W. M.: CRC Handbook of Chemistry and Physics, 96th ed., CRC Press/Taylor and Francis Group, Boca Raton, FL., 2015.

Heald, C. L., Kroll, J. H., Jimenez, J. L., Docherty, K. S., Decarlo, P. F., Aiken, A. C., Chen, Q., Martin, S. T., Farmer, D. K. and Artaxo, P.: A simplified description of the evolution of organic aerosol composition in the atmosphere, Geophys. Res. Lett., 37(8), L08803, doi:10.1029/2010GL042737, 2010.

~~Hinks, M. L., Brady, M. V, Lignell, H., Song, M., Grayson, J. W., Bertram, A., Lin, P., Laskin, A., Laskin, J. and Nizkorodov, S. A.: Effect of Viscosity on Photodegradation Rates in Complex Secondary Organic Aerosol Materials, Phys. Chem. Chem. Phys., 18(13), 8785–8793, doi:10.1039/C5CP05226B, 2016.~~

Hosny, N. A., Fitzgerald, C., Tong, C., Kalberer, M., Kuimova, M. K. and Pope, F. D.: Fluorescent lifetime imaging of atmospheric aerosols: a direct probe of aerosol viscosity, Faraday Discuss., 165, 343–356, doi:10.1039/c3fd00041a, 2013.

Huff Hartz, K. E., Rosenørn, T., Ferchak, S. R., Raymond, T. M., Bilde, M., Donahue, N. M. and Pandis, S. N.: Cloud condensation nuclei activation of monoterpene and sesquiterpene secondary organic aerosol, J. Geophys. Res. D Atmos., 110(14), 1–8, doi:10.1029/2004JD005754, 2005.

Jimenez, J. L., Canagaratna, M. R., Donahue, N. M., Prevot, A. S. H., Zhang, Q., Kroll, J. H., DeCarlo, P. F., Allan, J. D., Coe, H., Ng, N. L., Aiken, A. C., Docherty, K. S., Ulbrich, I. M., Grieshop, A. P., Robinson, A. L., Duplissy, J., Smith, J. D., Wilson, K. R., Lanz, V. A., Hueglin, C., Sun, Y. L., Tian, J., Laaksonen, A., Raatikainen, T., Rautiainen, J., Vaattovaara, P., Ehn, M., Kumala, M., Tomlinson, J. M., Collins, D. R., Cubison, M. J., Dunlea, E. J., Huffman, J. A., Onasch, T. B., Alfarra, M. R., Williams, P. I., Bower, K., Kondo, Y., Schneider, J., Drewnick, F., Borrmann, S., Weimer, S., Demerjian, K., Salcedo, D., Cottrell, L., Griffin, R., Takami, A., Miyoshi, T., Hatakeyama, S., Shimono, A., Sun, J. Y., Zhang, Y. M., Dzepina, K., Kimmel, J. R., Sueper, D., Jayne, J. T., Herndon, S. C., Trimborn, A. M., Williams, L. R., Wood, E. C., Middlebrook, A. M., Kolb, C. E., Baltensperger, U. and Worsnop, D. R.: Evolution of Organic Aerosols in the Atmosphere, Science (80-.)., 326(5959), 1525–1529, doi:10.1126/science.1180353, 2009.

Jöckel, P., Tost, H., Pozzer, A., Brühl, C., Buchholz, J., Ganzeveld, L., Hoor, P., Kerkweg, A., Lawrence, M. G., Sander, R., Steil, B., Stiller, G., Tanarhte, M., Taraborrelli, D., van Aardenne, J. and Lelieveld, J.: The atmospheric chemistry general circulation model ECHAM5/MESSy1: consistent simulation of ozone from the surface to the mesosphere, Atmos. Chem. Phys. Discuss., 6(4), 6957–7050, doi:10.5194/acp-6-5067-2006, 2006.

Koop, T., Bookhold, J., Shiraiwa, M. and Pöschl, U.: Glass transition and phase state of organic compounds: dependency on molecular properties and implications for secondary organic aerosols in the atmosphere, Phys. Chem. Chem. Phys., 13(43),

19238–19255, doi:10.1039/c1cp22617g, 2011.

Lakey, P. S. J., Berkemeier, T., Krapf, M., Dommen, J., Steimer, S. S., Whalley, L. K., Ingham, T., Baeza-Romero, M. T., Pöschl, U., Shiraiwa, M., Ammann, M. and Heard, D. E.: The effect of viscosity and diffusion on the HO2uptake by sucrose and secondary organic aerosol particles, Atmos. Chem. Phys., 16(20), 13035–13047, doi:10.5194/acp-16-13035-2016, 2016.

Laskin, J., Laskin, A. and Nizkorodov, S. A.: Mass Spectrometry Analysis in Atmospheric Chemistry, Anal. Chem., 90(1), 166–189, doi:10.1021/acs.analchem.7b04249, 2018.

Li, Y. J., Liu, P., Gong, Z., Wang, Y., Bateman, A. P., Bergoend, C., Bertram, A. K. and Martin, S. T.: Chemical reactivity and liquid/nonliquid states of secondary organic material, Environ. Sci. Technol., 49(22), 13264–13274, doi:10.1021/acs.est.5b03392, 2015.

Lide, D. R., Ed.: CRC Handbook of Chemistry and Physics, 82nd ed., CRC Press, Boca Raton, FL., 2001.

~~Lignell, H., Hinks, M. L. and Nizkorodov, S. A.: Exploring matrix effects on photochemistry of organic aerosols, Proc. Natl. Acad. Sci. U. S. A., 111(38), 13780–13785, doi:10.1073/pnas.1322106111, 2014.~~

Liu, P., Li, Y. J., Wang, Y., Gilles, M. K., Zaveri, R. A., Bertram, A. K. and Martin, S. T.: Lability of secondary organic particulate matter, Proc. Natl. Acad. Sci., 113(45), 12643–12648, doi:10.1073/pnas.1603138113, 2016.

Liu, P., Li, Y. J., Wang, Y., Bateman, A. P., Zhang, Y., Gong, Z., Bertram, A. K. and Martin, S. T.: Highly Viscous States Affect the Browning of Atmospheric Organic Particulate Matter, ACS Cent. Sci., 4(2), 207–215, doi:10.1021/acscentsci.7b00452, 2018.

Liu, S., Day, D. A., Shields, J. E. and Russell, L. M.: Ozone-driven daytime formation of secondary organic aerosol containing carboxylic acid groups and alkane groups, Atmos. Chem. Phys., 11(16), 8321–8341, doi:10.5194/acp-11-8321-2011, 2011.

Maclean, A. M., Butenhoff, C. L., Grayson, J. W., Barsanti, K., Jimenez, J. L. and Bertram, A. K.: Mixing times of organic molecules within secondary organic aerosol particles: A global planetary boundary layer perspective, Atmos. Chem. Phys., 17(21), 13037–13048, doi:10.5194/acp-17-13037-2017, 2017.

Marshall, F. H., Miles, R. E. H., Song, Y.-C., Ohm, P. B., Power, R. M., Reid, J. P. and Dutcher, C. S.: Diffusion and reactivity in ultraviscous aerosol and the correlation with particle viscosity, Chem. Sci., 7(2), 1298–1308, doi:10.1039/C5SC03223G, 2016.

Martin, S. T., Andreae, M. O., Althausen, D., Artaxo, P., Baars, H., Borrmann, S., Chen, Q., Farmer, D. K., Guenther, A., Gunthe, S. S., Jimenez, J. L., Karl, T., Longo, K., Manzi, A., Müller, T., Pauliquevis, T., Petters, M. D., Prenni, A. J., Pöschl, U., Rizzo, L. V., Schneider, J., Smith, J. N., Swietlicki, E., Tota, J., Wang, J., Wiedensohler, A. and Zorn, S. R.: An overview of the Amazonian Aerosol Characterization Experiment 2008 (AMAZE-08), Atmos. Chem. Phys., 10(23), 11415–11438, doi:10.5194/acp-10-11415-2010, 2010.

Migliori, M., Gabriele, D., Di Sanzo, R., De Cindio, B. and Correra, S.: Viscosity of multicomponent solutions of simple and complex sugars in water, J. Chem. Eng. Data, 52, 1347–1353, doi:10.1021/je700062x, 2007.

Miller, D. P., Anderson, R. E. and De Pablo, J. J.: Stabilization of lactate dehydrogenase following freeze-thawing and vacuum-drying in the presence of trehalose and borate, Pharm. Res., 15(8), 1215–1221, doi:10.1023/A:1011987707515, 1998.

Mu, Q., Shiraiwa, M., Octaviani, M., Ma, N., Ding, A., Su, H., Lammel, G., Pöschl, U. and Cheng, Y.: Temperature effect on phase state and reactivity controls atmospheric multiphase chemistry and transport of PAHs, Sci. Adv., 4(3), doi:10.1126/sciadv.aap7314, 2018.

Ng, N. L., Canagaratna, M. R., Zhang, Q., Jimenez, J. L., Tian, J., Ulbrich, I. M., Kroll, J. H., Docherty, K. S., Chhabra, P. S., Bahreini, R., Murphy, S. M., Seinfeld, J. H., Hildebrandt, L., Donahue, N. M., Decarlo, P. F., Lanz, V. A., Prévôt, A. S. H., Dinar, E., Rudich, Y. and Worsnop, D. R.: Organic aerosol components observed in Northern Hemispheric datasets from Aerosol Mass Spectrometry, Atmos. Chem. Phys., 10(10), 4625–4641, doi:10.5194/acp-10-4625-2010, 2010.

Nozière, B., Kalberer, M., Claeys, M., Allan, J., D'Anna, B., Decesari, S., Finessi, E., Glasius, M., Grgić, I., Hamilton, J. F., Hoffmann, T., Iinuma, Y., Jaoui, M., Kahnt, A., Kampf, C. J., Kourtchev, I., Maenhaut, W., Marsden, N., Saarikoski, S., Schnelle-Kreis, J., Surratt, J. D., Szidat, S., Szmigielski, R. and Wisthaler, A.: The Molecular Identification of Organic Compounds in the Atmosphere: State of the Art and Challenges, Chem. Rev., 115(10), 3919–3983, doi:10.1021/cr5003485, 2015.

Pajunoja, A., Malila, J., Hao, L., Joutsensaari, J., Lehtinen, K. E. J. and Virtanen, A.: Estimating the Viscosity Range of SOA Particles Based on Their Coalescence Time, Aerosol Sci. Technol., 48(2), doi:10.1080/02786826.2013.870325, 2014.

Pant, A., Parsons, M. T. and Bertram, A. K.: Crystallization of aqueous ammonium sulfate particles internally mixed with soot and kaolinite: Crystallization relative humidities and nucleation rates, J. Phys. Chem. A, 110(28), 8701–8709, doi:10.1021/jp060985s, 2006.

Perraud, V., Bruns, E. A., Ezell, M. J., Johnson, S. N., Yu, Y., Alexander, M. L., Zelenyuk, A., Imre, D., Chang, W. L., Dabdub, D., Pankow, J. F. and Finlayson-Pitts, B. J.: Nonequilibrium atmospheric secondary organic aerosol formation and growth, Proc. Natl. Acad. Sci. U. S. A., 109, 2836–2841, doi:10.1073/pnas.1119909109, 2012.

Pollack, G. L.: Atomic test of the Stokes-Einstein law: Diffusion and solubility of Xe, Phys. Rev. A, 23(5), 2660–2663, doi:10.1103/PhysRevA.23.2660, 1981.

Pöschl, U., Martin, S. T., Sinha, B., Chen, Q., Gunthe, S. S., Huffman, J. A., Borrmann, S., Farmer, D. K., Garland, R. M., Helas, G., Jimenez, J. L., King, S. M., Manzi, A., Mikhailov, E., Pauliquevis, T., Petters, M. D., Prenni, A. J., Roldin, P., Rose, D., Schneider, J., Su, H., Zorn, S. R., Artaxo, P. and Andreae, M. O.: Rainforest Aerosols as Biogenic Nuclei of Clouds and Precipitation in the Amazon, Science (80-.)., 329, 1513–1517, doi:10.1126/science.1191056, 2010.

Power, R. M., Simpson, S. H., Reid, J. P. and Hudson, A. J.: The transition from liquid to solid-like behaviour in ultrahigh viscosity aerosol particles, Chem. Sci., 4(6), 2597–2604, doi:10.1039/C3SC50682G, 2013.

Price, H. C., Murray, B. J., Mattsson, J., O'Sullivan, D., Wilson, T. W., Baustian, K. J. and Benning, L. G.: Quantifying water diffusion in high-viscosity and glassy aqueous solutions using a Raman isotope tracer method, Atmos. Chem. Phys. Discuss., 14, 3817–3830, doi:10.5194/acpd-13-29375-2013, 2014.

Price, H. C., Mattsson, J. and Murray, B. J.: Sucrose diffusion in aqueous solution, Phys. Chem. Chem. Phys., 18, 19207–19216, doi:10.1039/C6CP03238A, 2016.

Quintas, M., Brandão, T. R. S., Silva, C. L. M. and Cunha, R. L.: Rheology of supersaturated sucrose solutions, J. Food Eng.,

77(4), 844–852, doi:10.1016/j.jfoodeng.2005.08.011, 2006.

Rampp, M., Buttersack, C. and Luedemann, H. D.: c,T-dependence of the viscosity and the self-diffusion coefficients in some aqueous carbohydrate solutions, Carbohydr. Res., 328, 561–572, doi:10.1016/S0008-6215(00)00141-5, 2000.

Reid, J. P., Bertram, A. K., Topping, D. O., Laskin, A., Martin, S. T., Petters, M. D., Pope, F. D. and Rovelli, G.: The viscosity of atmospherically relevant organic particles, Nat. Commun., 9, 1–14, doi:10.1038/s41467-018-03027-z, 2018.

Renbaum-Wolff, L., Grayson, J. W., Bateman, A. P., Kuwata, M., Sellier, M., Murray, B. J., Shilling, J. E., Martin, S. T. and Bertram, A. K.: Viscosity of α-pinene secondary organic material and implications for particle growth and reactivity., Proc. Natl. Acad. Sci. U. S. A., 110(20), 8014–8019, doi:10.1073/pnas.1219548110, 2013.

Riipinen, I., Pierce, J. R., Yli-Juuti, T., Nieminen, T., Haekkinen, S., Ehn, M., Junninen, H., Lehtipalo, K., Petaejae, T., Slowik, J., Chang, R., Shantz, N. C., Abbatt, J., Leaitch, W. R., Kerminen, V. M., Worsnop, D. R., Pandis, S. N., Donahue, N. M. and Kulmala, M.: Organic condensation: A vital link connecting aerosol formation to cloud condensation nuclei (CCN) concentrations, Atmos. Chem. Phys., 11, 3865–3878, doi:10.5194/acp-11-3865-2011, 2011.

Rovelli, G., Song, Y. C., Maclean, A. M., Topping, D. O., Bertram, A. K. and Reid, J. P.: Comparison of Approaches for Measuring and Predicting the Viscosity of Ternary Component Aerosol Particles, Anal. Chem., 91, 5074–5082, doi:10.1021/acs.analchem.8b05353, 2019.

Saathoff, H., Naumann, K.-H., Möhler, O., Jonsson, Å. M., Hallquist, M., Kiendler-Scharr, A., Mentel, T. F., Tillmann, R. and Schurath, U.: Temperature dependence of yields of secondary organic aerosols from the ozonolysis of α-pinene and limonene, Atmos. Chem. Phys. Discuss., 8(4), 15595–15664, doi:10.5194/acpd-8-15595-2008, 2009.

Seinfeld, J. H. and Pandis, S. N.: Atmospheric Chemistry and Physics: From Air Pollution to Climate Change, Wiley-Interscience, Hoboken, New Jersey., 2006.

Shamblin, S. L., Tang, X., Chang, L., Hancock, B. C. and Pikal, M. J.: Characterization of the time scales of molecular motion in pharmaceutically important glasses, J. Phys. Chem. B, 103(20), 4113–4121, doi:10.1021/jp983964+, 1999.

Shiraiwa, M., Ammann, M., Koop, T. and Poschl, U.: Gas uptake and chemical aging of semisolid organic aerosol particles, Proc. Natl. Acad. Sci. U. S. A., 108(27), 11003–11008, doi:10.1073/pnas.1103045108, 2011.

Shiraiwa, M., Li, Y., Tsimpidi, A. P., Karydis, V. A., Berkemeier, T., Pandis, S. N., Lelieveld, J., Koop, T. and Pöschl, U.: Global distribution of particle phase state in atmospheric secondary organic aerosols, Nat. Commun., 8, 1–7, doi:10.1038/ncomms15002, 2017.

Shrivastava, M., Lou, S., Zelenyuk, A., Easter, R. C., Corley, R. A., Thrall, B. D., Rasch, P. J., Fast, J. D., Massey Simonich, S. L., Shen, H. and Tao, S.: Global long-range transport and lung cancer risk from polycyclic aromatic hydrocarbons shielded by coatings of organic aerosol, Proc. Natl. Acad. Sci., 114(6), 1246–1251, doi:10.1073/pnas.1618475114, 2017a.

Shrivastava, M., Cappa, C. D., Fan, J., Goldstein, A. H., Guenther, A. B., Jimenez, J. L., Kuang, C., Laskin, A., Martin, S. T., Ng, N. L., Petaja, T., Pierce, J. R., Rasch, P. J., Roldin, P., Seinfeld, J. H., Shilling, J., Smith, J. N., Thornton, J. A., Volkamer, R., Wang, J., Worsnop, D. R., Zaveri, R. A., Zelenyuk, A. and Zhang, Q.: Recent advances in understanding secondary organic aerosol: Implications for global climate forcing, Rev. Geophys., 55(2), 509–559, doi:10.1002/2016RG000540, 2017b.

van der Sman, R. G. M. and Meinders, M. B. J.: Moisture diffusivity in food materials, Food Chem., 138, 1265–1274, doi:http://dx.doi.org/10.1016/j.foodchem.2012.10.062, 2013.

Song, M., Liu, P. F., Hanna, S. J., Li, Y. J., Martin, S. T. and Bertram, A. K.: Relative humidity-dependent viscosities of isoprene-derived secondary organic material and atmospheric implications for isoprene-dominant forests, Atmos. Chem. Phys., 15(9), 5145–5159, doi:10.5194/acp-15-5145-2015, 2015.

Song, M., Liu, P. F., Hanna, S. J., Zaveri, R. A., Potter, K., You, Y., Martin, S. T. and Bertram, A. K.: Relative humidity-dependent viscosity of secondary organic material from toluene photo-oxidation and possible implications for organic particulate matter over megacities, Atmos. Chem. Phys., 16(14), 8817–8830, doi:10.5194/acp-16-8817-2016, 2016a.

Song, Y. C., Haddrell, A. E., Bzdek, B. R., Reid, J. P., Bannan, T., Topping, D. O., Percival, C. and Cai, C.: Measurements and predictions of binary component aerosol particle viscosity, J. Phys. Chem. A, 120(41), 8123–8137, doi:10.1021/acs.jpca.6b07835, 2016b.

Stocker, T. F., Qin, D., Plattner, G.-K., Tignor, M. M. B., Allen, S. K., Boschung, J., Nauels, A., Xia, Y., Bex, V. and Midgely, P. M., Eds.: IPCC Climate Change 2013: The Physical Science Basis. Contribution of Working Group I to the Fifth Assessment Report of the Intergovernmental Panel on Climate Change, Cambridge University Press, Cambridge, United Kingdom and New York, NY, USA., 2013.

Surratt, J. D., Murphy, S. M., Kroll, J. H., Ng, N. L., Hildebrandt, L., Sorooshian, A., Szmigielski, R., Vermeylen, R., Maenhaut, W., Claeys, M., Flagan, R. C. and Seinfeld, J. H.: Chemical composition of secondary organic aerosol formed from the photooxidation of isoprene, J. Phys. Chem. A, 110(31), 9665–9690, doi:10.1021/jp061734m, 2006.

Surratt, J. D., Chan, A. W., Eddingsaas, N. C., Chan, M., Loza, C. L., Kwan, a J., Hersey, S. P., Flagan, R. C., Wennberg, P. O. and Seinfeld, J. H.: Reactive intermediates revealed in secondary organic aerosol formation from isoprene, Proc. Natl. Acad. Sci. U. S. A., 107(15), 6640–6645, doi:10.1073/pnas.0911114107, 2010.

Swindells, J. F., Snyder, C. F., Hardy, R. C. and Golden, P. E.: Viscosities of sucrose solutions at various temperatures: Tables of recalculated values., 1958.

Takahama, S., Schwartz, R. E., Russell, L. M., MacDonald, A. M., Sharma, S. and Leaitch, W. R.: Organic functional groups in aerosol particles from burning and non-burning forest emissions at a high-elevation mountain site, Atmos. Chem. Phys., 11(13), 6367–6386, doi:10.5194/acp-11-6367-2011, 2011.

Telis, V. R. N., Telis-Romero, J., Mazzotti, H. B. and Gabas, A. L.: Viscosity of aqueous carbohydrate solutions at different temperatures and concentrations, Int. J. Food Prop., 10(1), 185–195, doi:10.1080/10942910600673636, 2007.

Tsimpidi, A. P., Karydis, V. A., Pozzer, A., Pandis, S. N. and Lelieveld, J.: ORACLE (v1.0): Module to simulate the organic aerosol composition and evolution in the atmosphere, Geosci. Model Dev., 7(6), 3153–3172, doi:10.5194/gmd-7-3153-2014, 2014.

Tsimpidi, A. P., Karydis, V. A., Pozzer, A., Pandis, S. N. and Lelieveld, J.: ORACLE 2-D (v2.0): An efficient module to compute the volatility and oxygen content of organic aerosol with a global chemistry-climate model, Geosci. Model Dev., 11(8), 3369–3389, doi:10.5194/gmd-11-3369-2018, 2018.

Ullmann, D. A., Hinks, M. L., Maclean, A., Butenhoff, C., Grayson, J., Barsanti, K., Jimenez, J. L., Nizkorodov, S. A., Kamal, S. and Bertram, A. K.: Viscosities, diffusion coefficients, and mixing times of intrinsic fluorescent organic molecules in brown limonene secondary organic aerosol and tests of the Stokes-Einstein equation, Atmos. Chem. Phys., 19, 1491–1503, doi:10.5194/acp-19-1491-2019, 2019.

Vaden, T. D., Imre, D., Beránek, J., Shrivastava, M. and Zelenyuk, A.: Evaporation kinetics and phase of laboratory and ambient secondary organic aerosol., Proc. Natl. Acad. Sci. U. S. A., 108(6), 2190–2195, doi:10.1073/pnas.1013391108, 2011.

Virtanen, A., Joutsensaari, J., Koop, T., Kannosto, J., Yli-Pirilä, P., Leskinen, J., Mäkelä, J. M., Holopainen, J. K., Pöschl, U., Kulmala, M., Worsnop, D. R. and Laaksonen, A.: An amorphous solid state of biogenic secondary organic aerosol particles, Nature, 467(7317), 824–827, doi:10.1038/nature09455, 2010.

Wheeler, M. J. and Bertram, A. K.: Deposition nucleation on mineral dust particles: A case against classical nucleation theory with the assumption of a single contact angle, Atmos. Chem. Phys., 12(2), 1189–1201, doi:10.5194/acp-12-1189-2012, 2012.

Ye, Q., Robinson, E. S., Ding, X., Ye, P., Sullivan, R. C. and Donahue, N. M.: Mixing of secondary organic aerosols versus relative humidity, Proc. Natl. Acad. Sci., 113(45), 12649–12654, doi:10.1073/pnas.1604536113, 2016.

Zaveri, R. A., Easter, R. C., Shilling, J. E. and Seinfeld, J. H.: Modeling kinetic partitioning of secondary organic aerosol and size distribution dynamics: Representing effects of volatility, phase state, and particle-phase reaction, Atmos. Chem. Phys., 14(10), 5153–5181, doi:10.5194/acp-14-5153-2014, 2014.

~~Zaveri, R. A., Shilling, J. E., Zelenyuk, A., Liu, J., Bell, D. M., D'Ambro, E. L., Gaston, C. J., Thornton, J. A., Laskin, A., Lin, P., Wilson, J., Easter, R. C., Wang, J., Bertram, A. K., Martin, S. T., Seinfeld, J. H. and Worsnop, D. R.: Growth Kinetics and Size Distribution Dynamics of Viscous Secondary Organic Aerosol, Environ. Sci. Technol., 52(3), 1191–1199, doi:10.1021/acs.est.7b04623, 2018.~~

Zelenyuk, A., Imre, D., Beránek, J., Abramson, E., Wilson, J. and Shrivastava, M.: Synergy between secondary organic aerosols and long-range transport of polycyclic aromatic hydrocarbons., Environ. Sci. Technol., 46(22), 12459–12466, doi:10.1021/es302743z, 2012.

Zhang, Y., Chen, Y., Lambe, A. T., Olson, N. E., Lei, Z., Craig, R. L., Zhang, Z., Gold, A., Onasch, T. B., Jayne, J. T., Worsnop, D. R., Gaston, C. J., Thornton, J. A., Vizuete, W., Ault, A. P. and Surratt, J. D.: Effect of the Aerosol-Phase State on Secondary Organic Aerosol Formation from the Reactive Uptake of Isoprene-Derived Epoxydiols (IEPOX), Environ. Sci. Technol. Lett., 5(3), 167–174, doi:10.1021/acs.estlett.8b00044, 2018.

Zhou, S., Shiraiwa, M., McWhinney, R. D., Pöschl, U. and Abbatt, J. P. D.: Kinetic limitations in gas-particle reactions arising from slow diffusion in secondary organic aerosol, Faraday Discuss., 165, 391, doi:10.1039/c3fd00030c, 2013.

Zhou, S., Hwang, B. C. H., Lakey, P. S. J., Zuend, A., Abbatt, J. P. D. and Shiraiwa, M.: Multiphase reactivity of polycyclic aromatic hydrocarbons is driven by phase separation and diffusion limitations, Proc. Natl. Acad. Sci., 116(24), 11658–11663, doi:10.1073/pnas.1902517116, 2019.

S1. Calculation of equilibration times

The time required for droplets to come to equilibrium with the surrounding water activity (a_w) was calculated using the following equation (Seinfeld and Pandis, 2006; Shiraiwa et al., 2011):

$$\tau_{diff,H20} = \frac{dp^2}{4\pi^2 D_{H2O}} \quad \text{(S1)}$$

where $\tau_{diff, H2O}$ is the characteristic mixing time of water due to molecular diffusion, d_p is the diameter of the droplet, and D_{H2O} is the diffusion coefficient of water in the matrix. A discussion of the values used for D_{H2O} in organic-water droplets follows. Diffusion coefficients of water in the organic matrices studied here are assumed to equal the diffusion coefficients of water in a sucrose matrix when the viscosity of the two matrices are equal. Diffusion coefficients for water in a sucrose matrix at a given viscosity were calculated using a parametrization for diffusion coefficients as a function of a_w from Price et al. (2016) and a parameterization for sucrose viscosity as a function of a_w from Grayson et al. (2017). Those diffusion coefficients were used as an estimate for diffusion coefficients of water in citric acid, sorbitol, and sucrose-citric acid at that same viscosity. The expected viscosity of citric acid, sorbitol, and sucrose-citric acid matrices at each a_w was calculated using viscosity-a_w parameterizations from ~~(~~Rovelli et al.~~,~~ (2019)~~Rovelli et al. (n.d.) ~~and Song et al. (2016) (Figs. S7-S9).

S2. Diffusion coefficients and viscosity data from literature sources

Figure 3a in the main text includes log (D) – log ($kT/6\pi R_H$) plotted as a function of log (η) for organics diffusing in sucrose and brown limonene SOA matrices. The following gives additional details on this data.

S2.1 Sucrose matrices

In Price et al. (2016) and Chenyakin et al. (2017) , diffusion coefficients were reported as a function of a_w. The a_w was converted to viscosity using the viscosity vs. a_w parameterization from Figure S1 in Grayson et al. (2017) for sucrose solutions. The experiments of Chenyakin et al. (2017) were performed at 294.5 K, and the experiments of Price et al. (2016) were performed at 296 K.

The diffusion coefficients of Champion et al. (1997) were reported as a function of experimental temperature (T) minus the glass transition temperature (T_g). Those data were digitized using Origin software. The sucrose mass fraction of the solution used for each measurement was also given. The T_g at each sucrose mass fraction was calculated, using the Gordon-Taylor equation and parameters provided by Champion et al. (1997). Next, the experimental temperature for each measurement was calculated using the reported T-T_g values and the calculated T_g. Only diffusion coefficients measured at temperatures of 292 – 298 K were used. The sucrose mass fraction was converted to a_w using the relation between sucrose mass fraction and a_w

given in Zobrist et al. (2011). Finally, viscosity was calculated using the relation between viscosity and a_w given in Grayson et al. (2017) for sucrose solutions.

Rampp et al. (2000) measured diffusion coefficients of sucrose as a function of temperature, but reported their results for sucrose-water solutions in terms of parameters for the Vogel-Tammann-Fulcher (VTF) equation:

$$D = D_0 e^{\left(-\frac{T_0 C}{T - T_0}\right)} \quad \text{(S2)}$$

where D is the diffusion coefficient (m^2/s), and D_0, T_0, and C are free parameters. D_0 represents the expected diffusion at some value T_0, and C is the fragility parameter. The VTF parameters were reported as a function of mass fraction sucrose. Using the VTF equation and the reported VTF parameters, we calculated a diffusion coefficient at a temperature of 295 K for each mass fraction sucrose they studied. Sucrose mass fraction was then converted to viscosity using the relation between sucrose mass fraction and a_w of Zobrist et al. (2011) and the relation between viscosity and a_w in sucrose solutions given in Grayson et al. (2017).

Diffusion coefficients of the fluorescent organic molecule fluorescein in a sucrose matrix have also been measured by Corti et al. (2008) in the temperature range of 292-298 K. However, diffusion coefficients measured by Corti et al. (2008) are not included in Fig. 3 of the main text because Price et al. (2016) has shown that these measurements are inconsistent with other literature measurements of large organics in sucrose matrices.

As mentioned above, the viscosity-a_w parameterization provided in Figure S1 in Grayson et al. (2017) was used to convert water activities to viscosities in sucrose-water matrices. Sucrose-water viscosity data in that parameterization come from several viscosity measurements (Först et al., 2002; Green and Perry, 2007; Haynes, 2015; Lide, 2001; Migliori et al., 2007; Power et al., 2013; Quintas et al., 2006; Swindells et al., 1958; Telis et al., 2007). All viscosity measurements were made at a temperature of 293 K.

S2.2 Matrices consisting of brown limonene SOA generated in the laboratory

Diffusion coefficients in brown limonene SOA are reported as a function of a_w in Ullmann et al. (2019). The viscosity of brown limonene SOA matrices as a function of a_w were also reported in that work. Both diffusion and viscosity measurements were performed at 294.5 K.

Tables

Table S1. Water activity (a_w) of the headspace above each saturated salt solution used for conditioning droplets of fluorescent organic-water solutions. The a_w was calculated from relative humidity (RH, a_w = RH/100), which was measured using a handheld hygrometer with an uncertainty of ± 2.5%.

Inorganic salt	Water activity (a_w)
Potassium acetate (CH_3COOK)	0.23
Potassium acetate (CH_3COOK)[a]	0.26
Potassium acetate (CH_3COOK)[a]	0.28
Magnesium chloride ($MgCl_2 \cdot 6H_2O$)	0.33
Potassium carbonate (K_2CO_3)	0.43
Calcium nitrate $Ca(NO_3)_2 \cdot 4H_2O$	0.51
Sodium bromide (NaBr)	0.57
Sodium chloride (NaCl)	0.75
Potasium chloride (KCl)	0.86

[a] Subsaturated solutions of potassium acetate were used to access water activities between 0.23 and 0.33.

Table S2~~1~~. Selected parameters used in preparing droplets containing rhodamine 6G in a citric acid matrix for rFRAP experiments and experimental~~measured~~ diffusion coefficients. $\tau_{diffusion,\ H2O}$ is the calculated characteristic mixing time for molecular diffusion of water in the droplets (see section S1 and Eq. (S1)). $t_{experimental}$ is the time used for conditioning the droplets at a given relative humidity.

a_w	Max diameter (µm)	$\tau_{diffusion,\ H2O}$ (calculated)	$t_{experimental}$	Log (η, Pa s) [a]	Diffusion coefficient (m^2/s)
0.23 ± 0.025	228	1 hour	4.2 days	2.92 ± 0.61	2.99 E-15 ± 2.55E-15
0.331 ± 0.025	628	2.89 hours	20 hours	1.82 ± 0.56	1.73E-14 ± 7.83 E-15
0.432 ± 0.025	656	0.75 hours	20 hours	0.85 ± 0.54	1.30 E-13 ± 2.53 E-14
0.514 ± 0.025	542	9.1 minutes	15 hours	0.16 ± 0.51	5.53 E-13 ± 1.26E-13
0.571 ± 0.025	828	8.7 minutes	15 hours	-0.30 ± 0.50	1.05 E-12 ± 1.13 E-13
0.732 ± 0.025	914	38 seconds	20 hours	-1.31 ± 0.47	1.07 E-11 ± 1.44 E-12
0.863 ± 0.025	1128	6 seconds	15 hours	-1.89 ± 0.47	3.14 E-11 ± 3.72 E-12

[a] The lower limit of viscosity was calculated using the upper limit of a_w with the lower 95% confidence band in Fig. S7, while upper limit of viscosity was calculated using the lower limit of a_w with the upper 95% confidence band in Fig. S7.

Table S3~~2~~. Selected parameters used in preparing droplets containing cresyl violet in a citric acid matrix for rFRAP experiments and experimental~~measured~~ diffusion coefficients. $\tau_{diffusion,\ H2O}$ is the calculated characteristic mixing time for molecular diffusion of water in the droplets (see section S1 and Eq. (S1)). $t_{experimental}$ is the time used for conditioning the droplets at a given relative humidity.

a_w	Max diameter (µm)	$\tau_{diffusion,\ H2O}$ (calculated)	$t_{experimental}$	Log (η, Pa s) [a]	Diffusion coefficient (m^2/s)
0.23 ± 0.025	171	35 minutes	16 days	2.92 ± 0.61	8.59 E-16 ± 3.60 E-16
0.331 ± 0.025	100	246 seconds	17 hours	1.82 ± 0.56	3.80 E-14 ± 1.30 E-14
0.432 ± 0.025	100	62 seconds	17 hours	0.85 ± 0.54	2.63 E-13 ± 1.41 E-13
0.514 ± 0.025	1286	51 minutes	116 hours	0.16 ± 0.51	3.98 E-13 ± 2.87 E-13
0.571 ± 0.025	1170	17 minutes	18 hours	-0.30 ± 0.50	1.10 E-12 ± 6.87 E-13
0.732 ± 0.025	671	20 seconds	15 days	-1.31 ± 0.47	6.17 E-12 ± 3.49 E-12

[a] The lower limit of viscosity was calculated using the upper limit of a_w with the lower 95% confidence band in Fig. S7, while upper limit of viscosity was calculated using the lower limit of a_w with the upper 95% confidence band in Fig. S7.

Table S4~~3~~. Selected parameters used in preparing droplets containing rhodamine 6G in a sorbitol matrix for rFRAP experiments and experimental~~measured~~ diffusion coefficients. $\tau_{diffusion,\ H2O}$ is the calculated characteristic mixing time for molecular diffusion of water in the droplets (see section S1 and Eq. (S1)). $t_{experimental}$ is the time used for conditioning the droplets at a given relative humidity.

a_w	Max diameter (µm)	$\tau_{diffusion,\ H2O}$ (calculated)	$t_{experimental}$	Log (η, Pa s) [a]	Diffusion coefficient ($\mu m^2/s$)
0.23 ± 0.025	742	63.5 hours	8 days	4.24 ± 0.78	1.65 E-17 ± 1.44 E-17
0.331 ± 0.025	770	20.1 hours	7 days	3.31 ± 0.63	9.62 E-17 ± 2.55 E-17
0.432 ± 0.025	828	7.7 hours	4 days	2.36 ± 0.53	1.96 E-14 ± 4.52E-15
0.514 ± 0.025	1142	5.7 hours	4 days	1.61 ± 0.50	1.15 E-13 ± 3.24 E-14
0.571 ± 0.025	1000	2.2 hours	18 hours	1.05 ± 0.51	1.88E-13 + 2.17 E-14

a The lower limit of viscosity was calculated using the upper limit of a_w with the lower 95% confidence band in Fig. S8, while upper limit of viscosity was calculated using the lower limit of a_w with the upper 95% confidence band in Fig. S8.

Table S5~~4~~. Selected parameters used in preparing droplets containing rhodamine 6G in a sucrose-citric acid matrix for rFRAP experiments and experimental~~measured~~ diffusion coefficients. $\tau_{diffusion,\ H2O}$ is the calculated characteristic mixing time for molecular diffusion of water in the droplets (see section S1 and Eq. (S1)). $t_{experimental}$ is the time used for conditioning the droplets at a given relative humidity.

a_w	Max diameter (μm)	$\tau_{diffusion, H2O}$ (calculated)	$t_{experimental}$	Log (η, Pa s) [a]	Diffusion coefficient (m^2/s)
0.14 ± 0.025	243	60 hours	216 hours	6.60 ± 1.15	3.79E-19 ± 2.75 E-19
0.23 ± 0.025	685	60 hours	168 hours	4.92 ± 0.98	1.17 E-18 ± 9.72 E-19
0.26 ± 0.025	257	8.8 hours	72 hours	4.38 ± 0.93	6.23 E-17 ± 5.83 E-17
0.282 ± 0.025	385	13.7 hours	87 hours	4.03 ± 0.89	1.22 E-16 ± 6.49 E-17
0.331 ± 0.025	600	13.4 hours	576 hours	3.26 ± 0.82	4.78 E-16 ± 2.31 E-16
0.432 ± 0.025	571	2.2 hours	601 hours	1.82 ± 0.71	4.08 E-15 ± 1.15 E-15
0.514 ± 0.025	514	28 minutes	19 hours	0.82 ± 0.64	4.84 E-14 ± 1.52 E-14
0.571 ± 0.025	714	20.5 minutes	19 hours	0.16 ± 0.60	1.61 E-13 ± 1.24 E-14
0.732 ± 0.025	657	52 seconds	19 hours	-1.22 ± 0.60	2.85 E-12 ± 3.88 E-13
0.863 ± 0.025	685	13 seconds	19 hours	-1.94 ± 0.67	1.90 E-11 ± 2.00 E-12

[a] The lower limit of viscosity was calculated using the upper limit of a_w with the lower 95% confidence band in Fig. S9, while upper limit of viscosity was calculated using the lower limit of a_w with the upper 95% confidence band in Fig. S9.

Table S65. Hydrodynamic radii of diffusing organic molecules and matrix molecules used in this study.

Diffusing or matrix species	Organic Molecule	Radius (Å)	Reference
Diffusing	Fluorescein	5.02	(Mustafa et al., 1993)
	Rhodamine 6G	5.89	(Müller and Loman, 2008)
	Calcein	7.4	(Tamba et al., 2010)
	Cresyl violet	3.7	Molecular radius calculated using Van der Waals theory of atomic increments (Edward, 1970)
Diffusing and matrix	Sucrose	4.5	Based on the density of amorphous sucrose (Chenyakin et al., 2017)
	Brown limonene SOA components	5.4 ± 0.9	(Ullmann et al., 2019)
Matrix	Citric acid	3.7	(Müller and Stokes, 1956)
	Sorbitol	3.6	(Comper, 1996)

Figures

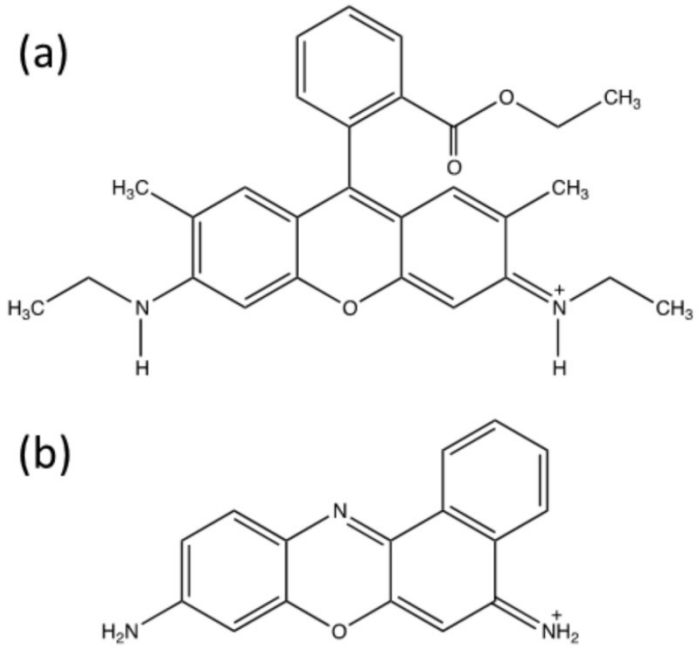

Figure S1. Chemical structures (protonated form) of the fluorescent organic molecules used in this study: A) rhodamine 6G and B) cresyl violet.

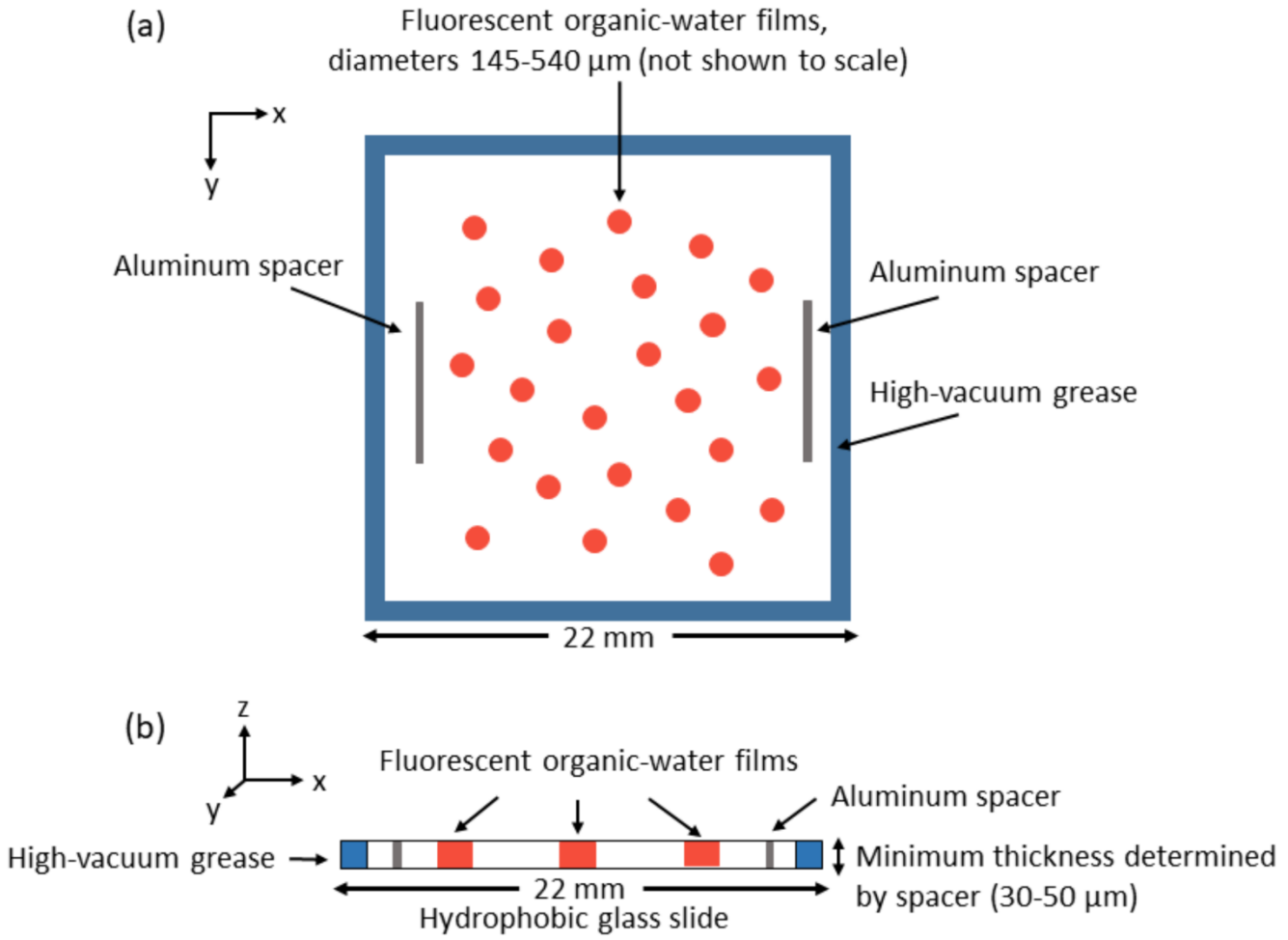

Figure S2. Top view (panel A) and side view (panel B) of a thin film of an organic-water matrix containing trace amounts of the fluorescent organic molecules, sandwiched between two hydrophobic glass slides, for use in rFRAP experiments.

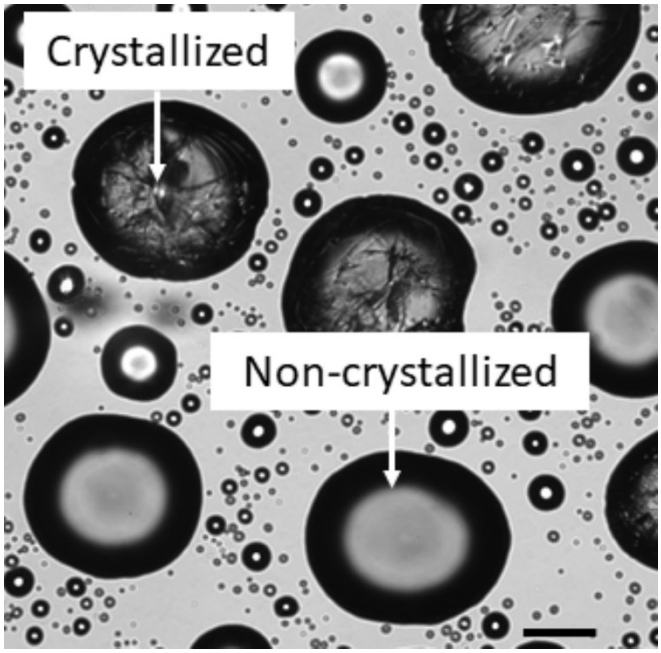

Figure S3. Image showing the difference between crystallized and non-crystallized droplets taken using an optical microscope. The sample was generated using a 0.08 mM solution of cresyl violet in a citric acid matrix, conditioned to $a_w = 0.26$. Slides with crystallized droplets were not used in rFRAP experiments.

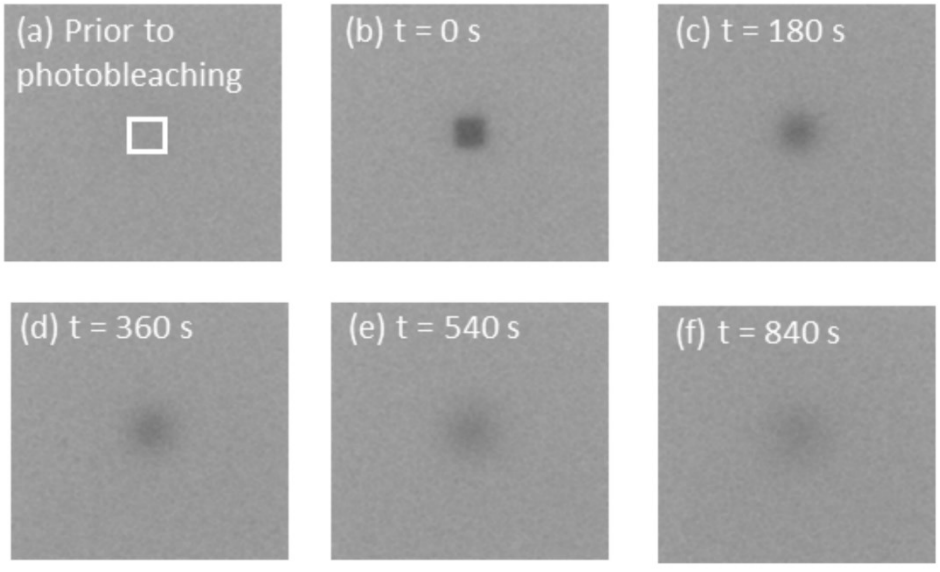

Figure S4. Fluorescence images of films containing rhodamine 6G, citric acid, and water at $a_w = 0.33$, collected using a confocal laser scanning microscope during a rFRAP experiment. Image (a) was taken prior to photobleaching and is used to normalize all images after photobleaching. Image (b) was taken immediately following the photobleaching event and images (c-f) were taken during the recovery period. The white square in panel A represents a 36 μm^2 region for photobleaching, while the size of the imaged region is 3600 μm^2.

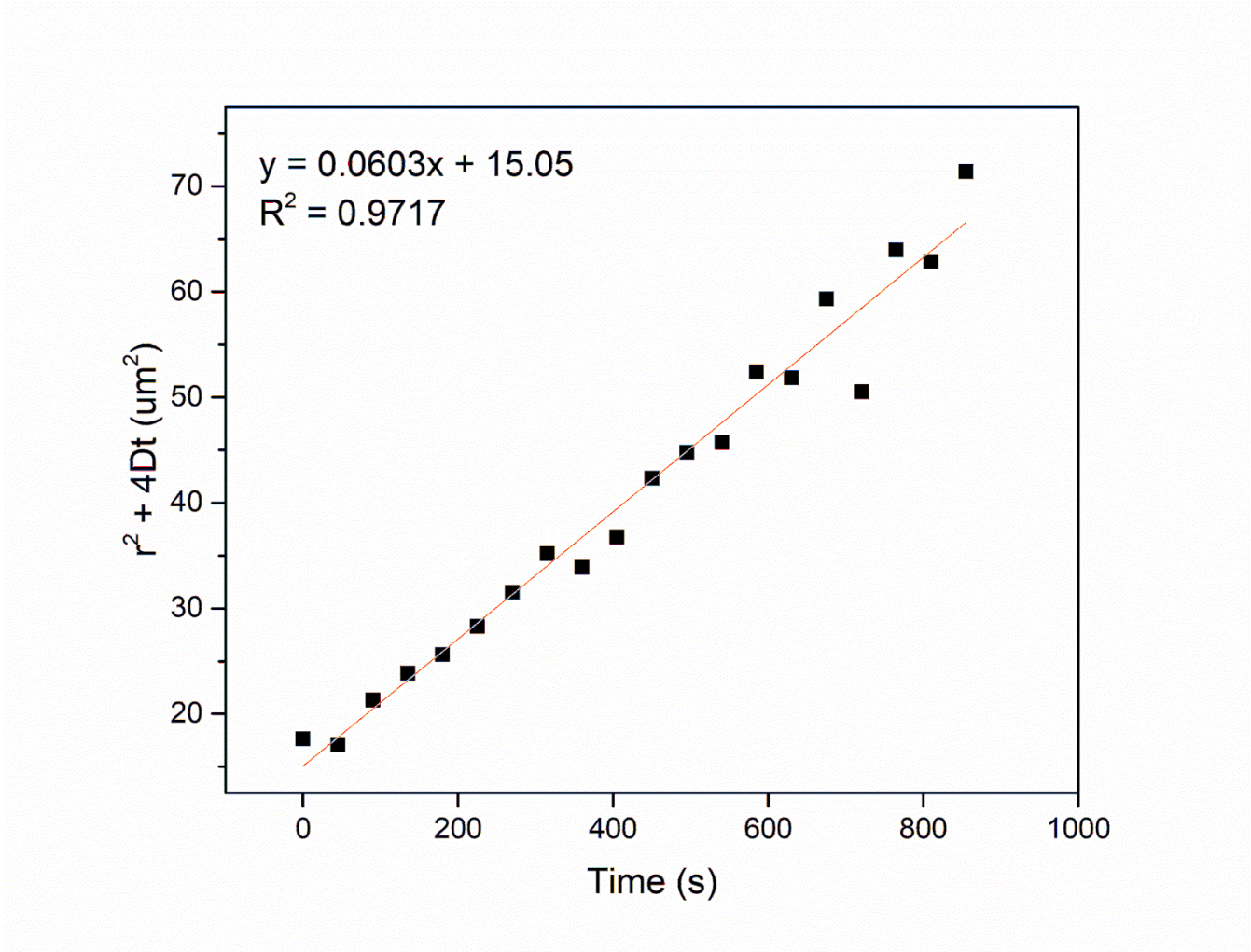

Figure S5. A plot of r^2+4Dt as a function of time after photobleaching in a sample of rhodamine 6G in citric acid matrix at $a_w = 0.33$. Each black square represents a value of r^2+4Dt from the fit of Eq. (2) to an image recorded after photobleaching. The red line is a linear best fit to the data.

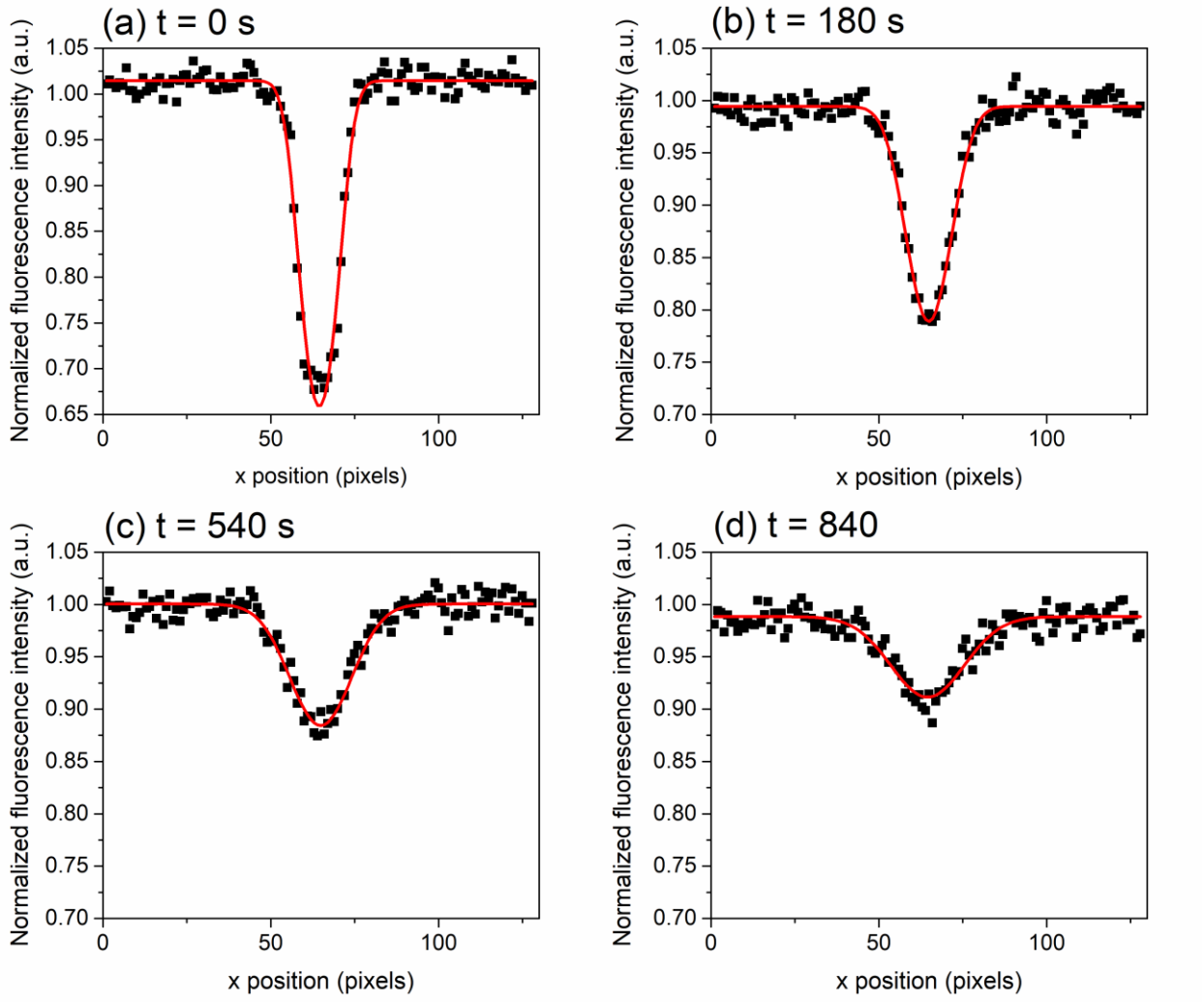

Figure S6. Cross-sectional view of the fluorescence intensity along the *x* direction for the fluorescence images shown in Fig. S4. To generate these plots, at each *x* position the fluorescence intensity is averaged over the width of the photobleached region in the *y* direction. The black squares represent measured fluorescence intensities, while the red line represents the calculated fit to the data. (a) shows the cross-sectional view immediately following the photobleaching event ($t = 0$ s), while (b-d) show the cross-sectional views during fluorescence recovery, at $t = 180$, 540, and 840 s.

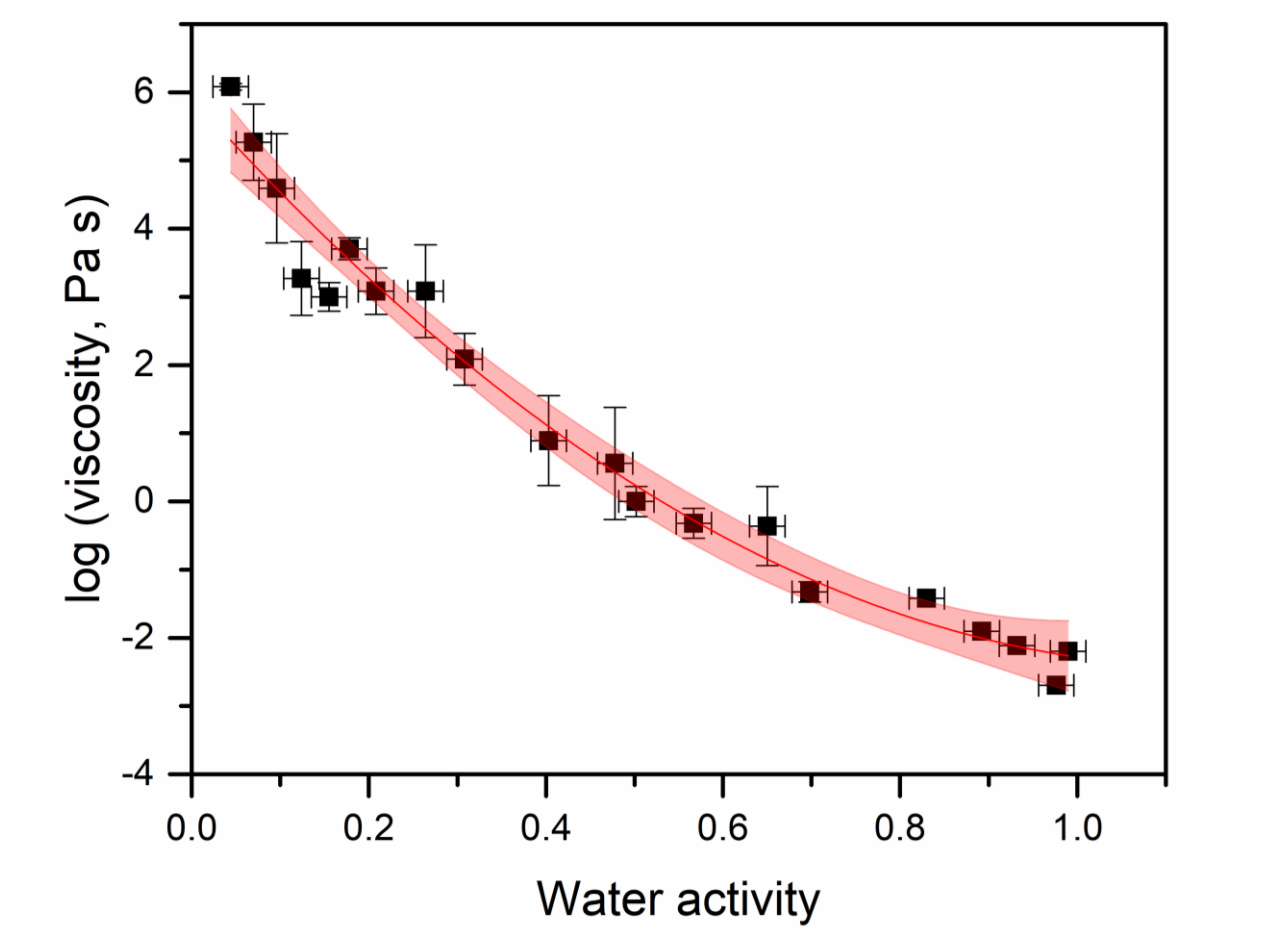

Figure S7. Parameterization between viscosity and water activity for citric acid solutions. Data come from Song et al. (2016) and include measurements on particles using the optical tweezers technique and measurements in the bulk phase using a rheometer. Measurements were performed at 293 ± 2 K. The equation of the second order polynomial line (red line) is log (η) = 5.9232 ± 0.3772 – 14.508 ± 0.3124(a_w) + 6.30235 ± 0.3605(a_w^2). X-error bars on the data points represent the ± 0.02 a_w and y-error bars represent one standard deviation calculated based on multiple viscosity measurements. Uncertainty in the parameterization (red shaded region) represent 95% confidence intervals.

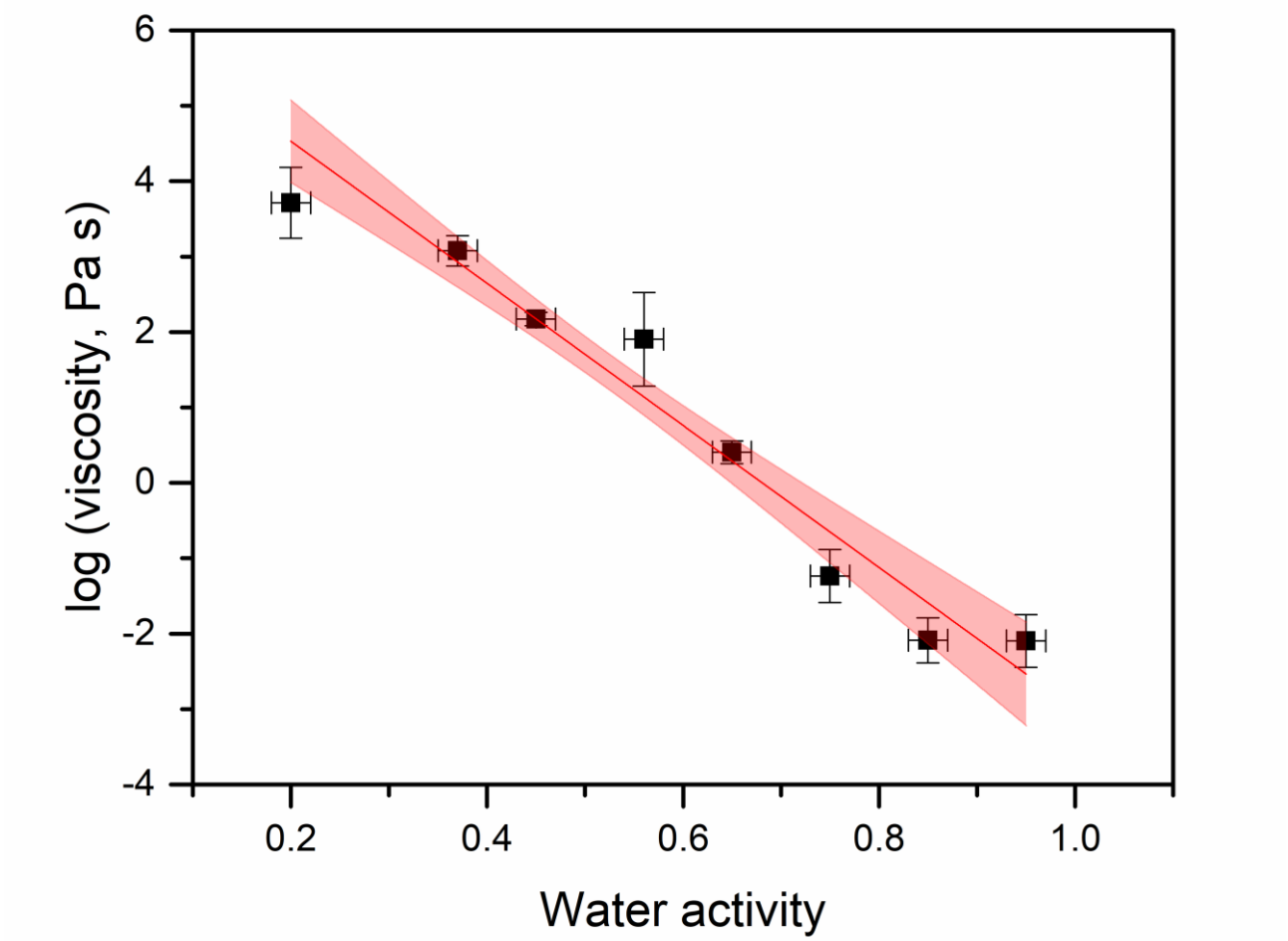

Figure S8. Parameterization between viscosity and water activity for sorbitol solutions. Data come from Song et al. (2016) and include measurements on particles using the optical tweezers technique. Measurements were performed at 293 ± 2 K. The equation of the line (red line) is log (η) = 6.4134 ± 1.021 – 9.4175 ± 2.871(a_w) + 0 ± 2.708(a_w^2). X-error bars on the data points represent the ± 0.02 a_w and y-error bars represent one standard deviation calculated based on multiple viscosity measurements. Uncertainty in the parameterization (red shaded region) represent 95% confidence intervals.

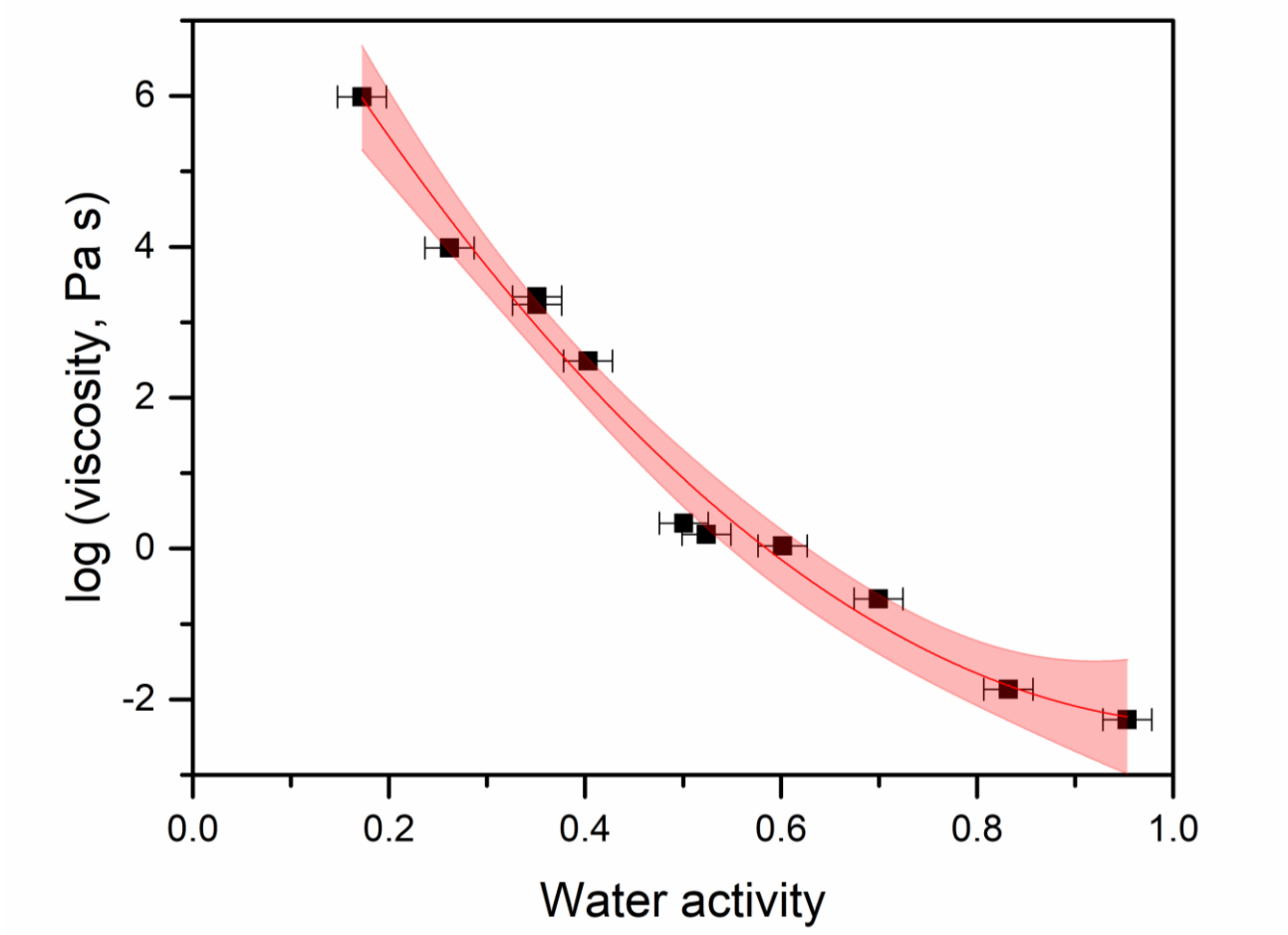

Figure S9. Parameterization between viscosity and water activity for sucrose-citric acid solutions. Data come from (Rovelli et al.**,** (2019)**Rovelli et al. (n.d.)** **and only include measurements on particles using the optical tweezers technique. Measurements performed using the poke-and-flow technique were not included due to the larger uncertainty in viscosity measurements using that technique. Measurements were performed at 293 ± 2 K. The equation of the line (red line) is log (η) = 9.55 ± 0.857 – 22.62 ± 1.97(a_w) + 10.76 ± 1.87(a_w^2). X-error bars on the data points represent the ± 0.02 a_w and y-error bars represent one standard deviation calculated based on multiple viscosity measurements. Uncertainty in the parameterization (red shaded region) represent 95% confidence intervals.**

References

Champion, D., Hervet, H., Blond, G., LeMeste, M. and Simatos, D.: Translational diffusion in sucrose solutions in the vicinity of their glass transition temperature, J. Phys. Chem. B., 101, 10674–10679, doi:10.1021/jp971899i, 1997.

Chenyakin, Y., Ullmann, D. A., Evoy, E., Renbaum-Wolff, L., Kamal, S. and Bertram, A. K.: Diffusion coefficients of organic molecules in sucrose-water solutions and comparison with Stokes-Einstein predictions, Atmos. Chem. Phys., 17, 2423–2435, doi:10.5194/acp-17-2423-2017, 2017.

Comper, W. D.: Extracellular Matrix Volume I: Tissue Function, Harwood Academic Publisher GmbH, Amsterdam., 1996.

Corti, H. R., Frank, G. A. and Marconi, M. C.: An alternate solution of fluorescence recovery kinetics after spot-bleaching for measuring diffusion coefficients. 2. Diffusion of fluorescein in aqueous sucrose solutions, J. Solution Chem., 37(11), 1593–1608, doi:10.1007/s10953-008-9329-4, 2008.

Edward, J. T.: Molecular volumes and the Stokes-Einstein equation, J. Chem. Educ., 47(4), 261, doi:10.1021/ed047p261, 1970.

Först, P., Werner, F. and Delgado, A.: On the pressure dependence of the viscosity of aqueous sugar solutions, Rheol. Acta, 41(4), 369–374, doi:10.1007/s00397-002-0238-y, 2002.

Grayson, J. W., Evoy, E., Song, M., Chu, Y., Maclean, A., Nguyen, A., Upshur, M. A., Ebrahimi, M., Chan, C. K., Geiger, F. M., Thomson, R. J. and Bertram, A. K.: The effect of hydroxyl functional groups and molar mass on the viscosity of non-crystalline organic and organic-water particles, Atmos. Chem. Phys., 17(13), 8509–8524, doi:10.5194/acp-17-8509-2017, 2017.

Green, D. W. and Perry, R. H.: Perry's Chemical Engineers' Handbook, 8th ed., The McGraw-Hill Companies, New York, NY., 2007.

Haynes, W. M.: CRC Handbook of Chemistry and Physics, 96th ed., CRC Press/Taylor and Francis Group, Boca Raton, FL., 2015.

Lide, D. R., Ed.: CRC Handbook of Chemistry and Physics, 82nd ed., CRC Press, Boca Raton, FL., 2001.

Migliori, M., Gabriele, D., Di Sanzo, R., De Cindio, B. and Correra, S.: Viscosity of multicomponent solutions of simple and complex sugars in water, J. Chem. Eng. Data, 52, 1347–1353, doi:10.1021/je700062x, 2007.

Müller, C. and Loman, A.: Precise measurement of diffusion by multi-color dual-focus fluorescence correlation spectroscopy, EPL, 83(4), 46001, doi:10.1209/0295-5075/83/46001, 2008.

Müller, T. A. and Stokes, R. H.: The mobility of the undissociated citric acid molecule in aqueous solution, Trans. Faraday Soc., 53, 642–645, 1956.

Mustafa, M. B., Tipton, D. L., Barkley, M. D., Russo, P. S. and Blum, F. D.: Dye diffusion in isotropic and liquid-crystalline aqueous (hydroxypropyl)cellulose, Macromolecules, 26(2), 370–378, doi:10.1021/ma00054a017, 1993.

Power, R. M., Simpson, S. H., Reid, J. P. and Hudson, A. J.: The transition from liquid to solid-like behaviour in ultrahigh viscosity aerosol particles, Chem. Sci., 4(6), 2597–2604, doi:10.1039/C3SC50682G, 2013.

Price, H. C., Mattsson, J. and Murray, B. J.: Sucrose diffusion in aqueous solution, Phys. Chem. Chem. Phys., 18, 19207–19216, doi:10.1039/C6CP03238A, 2016.

Quintas, M., Brandão, T. R. S., Silva, C. L. M. and Cunha, R. L.: Rheology of supersaturated sucrose solutions, J. Food Eng., 77(4), 844–852, doi:10.1016/j.jfoodeng.2005.08.011, 2006.

Rampp, M., Buttersack, C. and Luedemann, H. D.: c,T-dependence of the viscosity and the self-diffusion coefficients in some aqueous carbohydrate solutions, Carbohydr. Res., 328, 561–572, doi:10.1016/S0008-6215(00)00141-5, 2000.

Rovelli, G., Song, Y. C., Maclean, A. M., Topping, D. O., Bertram, A. K. and Reid, J. P.: Comparison of Approaches for Measuring and Predicting the Viscosity of Ternary Component Aerosol Particles, Anal. Chem., 91, 5074–5082, doi:10.1021/acs.analchem.8b05353, 2019.

Seinfeld, J. H. and Pandis, S. N.: Atmospheric Chemistry and Physics: From Air Pollution to Climate Change, Wiley-Interscience, Hoboken, New Jersey., 2006.

Shiraiwa, M., Ammann, M., Koop, T. and Poschl, U.: Gas uptake and chemical aging of semisolid organic aerosol particles, Proc. Natl. Acad. Sci. U. S. A., 108(27), 11003–11008, doi:10.1073/pnas.1103045108, 2011.

Song, Y. C., Haddrell, A. E., Bzdek, B. R., Reid, J. P., Bannan, T., Topping, D. O., Percival, C. and Cai, C.: Measurements and predictions of binary component aerosol particle viscosity, J. Phys. Chem. A, 120(41), 8123–8137, doi:10.1021/acs.jpca.6b07835, 2016.

Swindells, J. F., Snyder, C. F., Hardy, R. C. and Golden, P. E.: Viscosities of sucrose solutions at various temperatures: Tables of recalculated values., 1958.

Tamba, Y., Ariyama, H., Levadny, V. and Yamazaki, M.: Kinetic pathway of antimicrobial peptide magainin 2-induced pore formation in lipid membranes, J. Phys. Chem. B, 114(37), 12018–12026, doi:10.1021/jp104527y, 2010.

Telis, V. R. N., Telis-Romero, J., Mazzotti, H. B. and Gabas, A. L.: Viscosity of aqueous carbohydrate solutions at different temperatures and concentrations, Int. J. Food Prop., 10(1), 185–195, doi:10.1080/10942910600673636, 2007.

Ullmann, D. A., Hinks, M. L., Maclean, A., Butenhoff, C., Grayson, J., Barsanti, K., Jimenez, J. L., Nizkorodov, S. A., Kamal, S. and Bertram, A. K.: Viscosities, diffusion coefficients, and mixing times of intrinsic fluorescent organic molecules in brown limonene secondary organic aerosol and tests of the Stokes-Einstein equation, Atmos. Chem. Phys., 19, 1491–1503, doi:10.5194/acp-19-1491-2019, 2019.

Zobrist, B., Soonsin, V., Luo, B. P., Krieger, U. K., Marcolli, C., Peter, T. and Koop, T.: Ultra-slow water diffusion in aqueous sucrose glasses., Phys. Chem. Chem. Phys., 13, 3514–3526, doi:10.1039/c0cp01273d, 2011.